Title
THE A1 AND K(1320) PHENOMENA -- KINEMATIC ENHANCEMENTS OR MESONS?

Authors
Goldhaber, Gerson
Goldhaber, Sulamith.

Publication Date
1966-03-01

University of California

Ernest O. Lawrence Radiation Laboratory

THE A_1 AND K^*(1320) PHENOMENA KINEMATIC ENCHANCEMENTS OR MESONS ?

Berkeley, California

DISCLAIMER

UCRL-16744

Cy 4

Cy 4

Proc. 4th Anniv. Symposium
Inst. Math. Sci., Madras, India
January 3 to 11, 1966.

UNIVERSITY OF CALIFORNIA
Lawrence Radiation Laboratory
Berkeley, California

AEC Contract No. W-7405-eng-48

THE A_1 AND K^{**}(1320) PHENOMENA--KINEMATIC ENHANCEMENTS OR MESONS?

Gerson Goldhaber and Sulamith Goldhaber

March 1966

This article is based on the lecture notes prepared by the authors for the 4th Anniversary Symposium on Resonant States of Elementary Particles, held at the Institute of Mathematical Sciences, Madras, India, on January 3 to 11, 1966. Due to unforeseen circumstances these lectures were never presented.

The article is to be published in the Proceedings of the 4th Anniversary Symposium.

The A_1 and $K^{**}(1320)$ Phenomena-- Kinematic Enhancements or Mesons?

Gerson Goldhaber and Sulamith Goldhaber*

Lawrence Radiation Laboratory and Department of Physics
University of California, Berkeley, California

March 1966

INTRODUCTION

In this article we discuss the similarity, down to some very fine details, between the well-known A_1 phenomenon and the more recently discovered $K^{**}(1320)$ phenomenon. We wish to point out that this similarity is truly remarkable and can hardly be coincidental.

We will try to present the pros and cons, to the extent they are known to us, for the assignments of "kinematic enhancement" or "meson" to the A_1 and $K^{**}(1320)$ respectively. In view of the similarity between them we feel that when the ultimate decisions as to their identity can be made they may well turn out to be the same type of physical phenomena, namely either both kinematic enhancements or both mesons.

*Deceased. Sulamith Goldhaber died suddenly on December 11, 1965. At the time she was holding a Guggenheim Fellowship and the appointment of Visiting Professor at the Institute of Mathematical Sciences in Madras, India.

I. THE EXPERIMENTAL EVIDENCE FOR THE A_1 PHENOMENON

Before we comment on the subtle features involved in the A_1 let us review the current evidence for this phenomenon. The A_1 has been observed in four distinct experimental situations. These are:

(a) High momentum, 12 to 18 BeV/c, π^- interactions with complex nuclei in a heavy liquid bubble chamber.

(b) The reactions

$$\pi^{\pm} p \rightarrow \rho^0 \pi^{\pm} p$$

in the momentum intervals 2.75 to 4 BeV/c observed in hydrogen bubble chambers.

(c) The reaction

$$\pi^+ p \rightarrow \rho^0 \pi^+ p \text{ at 8 BeV/c and } \pi^- p \rightarrow \rho^0 \pi^- p$$

at 6 BeV/c in hydrogen bubble chambers.

(d) High momentum, 17 BeV/c, π^- interactions in photographic emulsions.

We will now consider these groups of experiments in turn:

(a). In a series of experiments studying the $\pi^-\pi^-\pi^+$ production, without visible nucleon excitation, using the Ecole Polytechnique heavy liquid bubble chamber at CERN, Allard et al.[1] have observed a very marked peak in the $\pi^-\pi^-\pi^+$ mass at 1.08 BeV. Furthermore, they find that if they limit their sample to events with low four-momentum transfer to the nucleus, nearly the entire A_1 peak is associated with ρ^0 formation (see Fig. 1). This is in accord with the decay mode $A_1^{\pm} \rightarrow \pi^{\pm} \rho^0$ discovered in the experiments with hydrogen.[2-4] No appreciable A_2 formation is observed in the data on complex nuclei.

(b). In Fig. 2 we show a recent compilation of the data in the 3- to 4-BeV/c region. For these data events with ρ^0 formation have been selected and the N^{*++} band has been removed. Here both the A_1 and A_2 peaks are observed, although A_2 formation is much more prominent than A_1 formation. Figure 3 shows the data of Alitti et al.[5] (SOBB Collaboration) at 2.75 BeV/c, which is not included in the above compilation. Alitti et al. also have reasonably good evidence for the $\rho^-\pi^0$ decay mode as well as the $\rho^0\pi^-$ decay mode of both the A_1 and A_2. If one were to characterize the

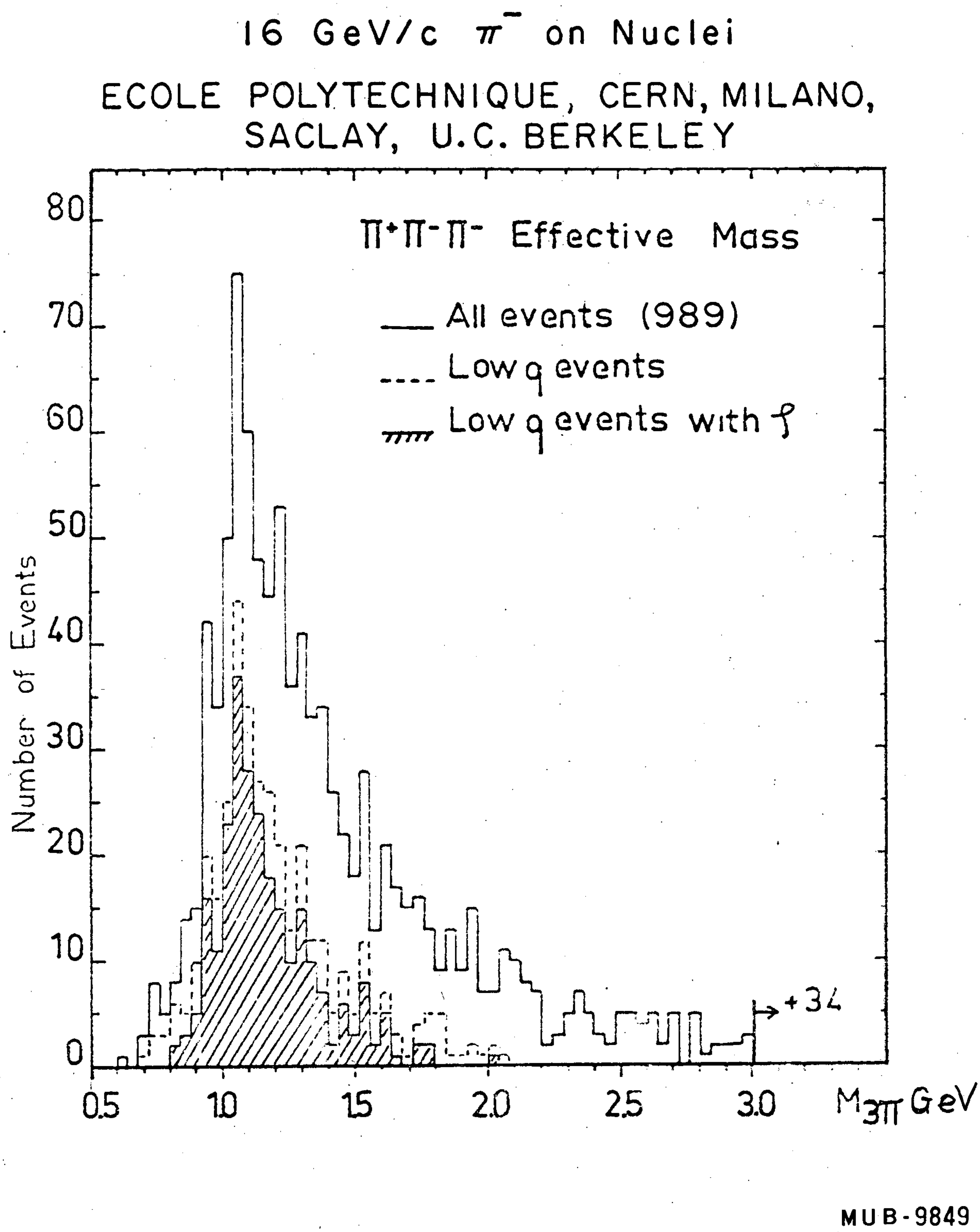

Fig. 1. The three-pion mass distribution from the heavy-liquid chamber experiment.

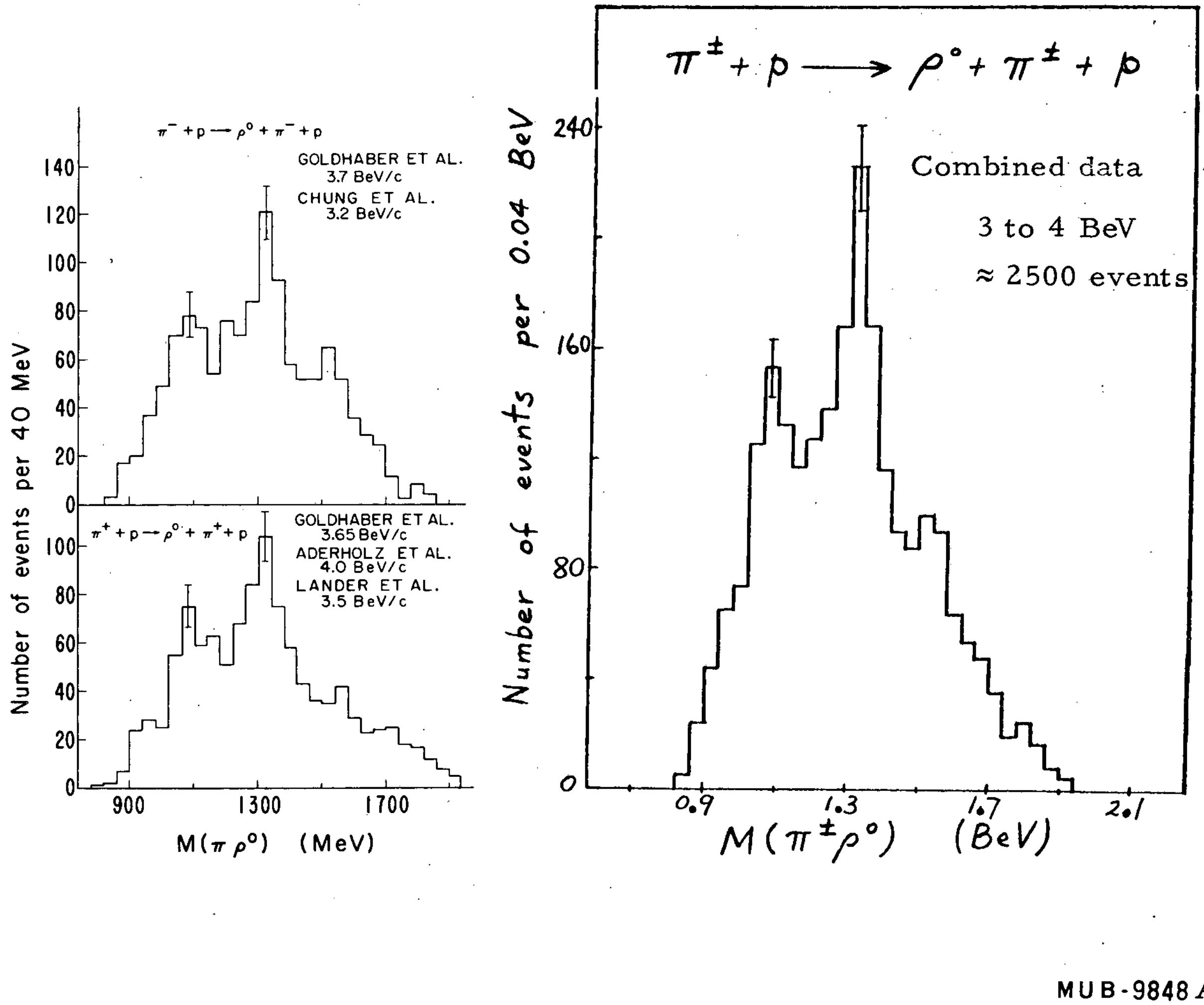

Fig. 2. Compilation of the $\pi^{\pm}\rho^{0}$ mass distribution from the available data in the 3- to 4-BeV/c region. The N^{*++} events have been removed in these plots.

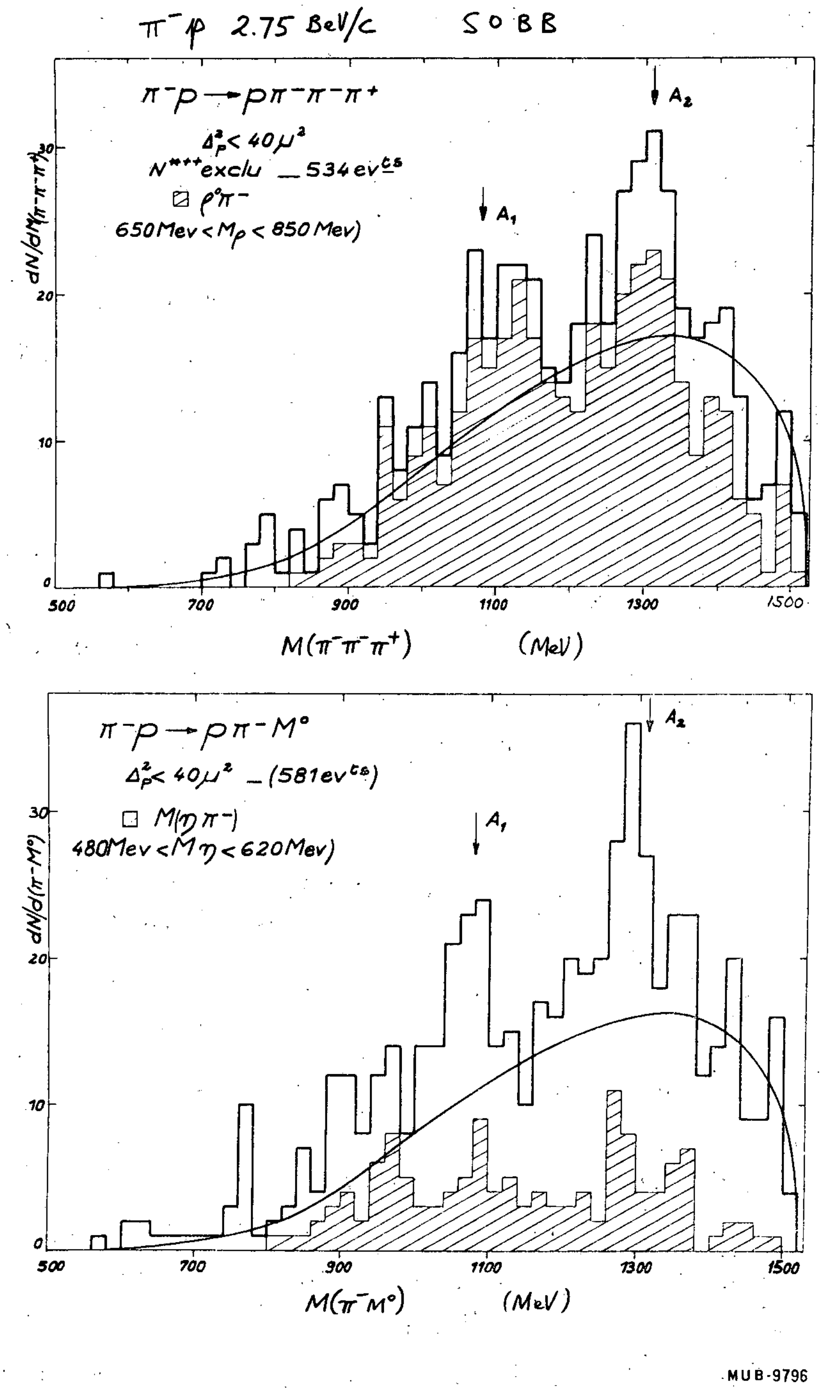

Fig. 3. (upper) The $\pi^-\pi^-\pi^+$ mass distribution from the π^-p interaction at 2.75 BeV/c. The shaded area corresponds to $\rho^0\pi^-$ events.

(lower) The π^-+ missing-mass distribution. The shaded area corresponds to $\pi\eta$ events.

$A^{\pm}$ phenomenon in the 2.75- to 4-BeV/c momentum interval in words, it could be described as a broad "pedestal" ranging roughly from 1.0 to 1.4 BeV in the $\pi^{\pm}\rho^{0}$ mass. At the upper end of this pedestal sits a very prominent A_2 peak at ≈ 1320 MeV (although the 6-BeV/c data[6] suggest $M(A_2)$ = 1290 MeV and the 8-BeV/c data[7] $M(A_2)$ = 1280 MeV). At the lower end of the pedestal a less prominent A_1 peak at ≈ 1080 MeV may be noted.

(c) The π^+p 8-BeV/c data,[7] taken at face value, appear to give two very clear-cut peaks, A_1 and A_2, of nearly comparable intensities and with a very definite separation between them (see Fig. 4). On the other hand the very recent data of Barnes et al., π^-p at 6 BeV/c,[6] with about half as many events, do not show any evidence for a distinct A_1 peak (see Fig. 4). Although the statistical accuracy of the two experiments is such that we are not really dealing with a serious discrepancy, it does make one wonder, however, whether the truth might not lie somewhere in between.

(d) The data of Bozóki et al.[8] from photographic emulsions are given in Fig. 5. These data show a distinct three-pion peak. The data confirm the production of a peak from interactions on complex nuclei, and are compared with a diffraction dissociation model.[9] No information is available from this experiment on the finer details we shall discuss subsequently.

II. THE EXPERIMENTAL EVIDENCE FOR THE $K^{**}(1320)$ PHENOMENON

Indications for a $K^{**}(1320)$ enhancement were first observed by Almeida et al.[10] in the K^+p reaction at 5 BeV/c. The effect is strongly reminiscent of the A enhancement. It was observed in the reaction $K^+p \rightarrow K^+\pi^-\pi^+p$.

One observes no striking enhancement if one looks at the <u>entire</u> $K^+\pi^-\pi^+$ mass distribution. However, if one selects the events with the $K^+\pi^-$ in the $K^{*0}(890)$ band one observes a clear-cut band on a Dalitz plot for the "three-particle" system $K^{*0}\pi^+p$. Furthermore, the projection of this Dalitz plot on the $K^{*0}\pi^+$ mass axis shows a peak centered at 1320 MeV, when the $N^{*++}(1238)$ band is removed. Here the K^{*0} is the SU(3) analog of the ρ^0, which occurs in the case of the A_1 enhancement. Figure 6 shows the data of Almeida et al., who obtained 41 events <u>after</u> the above two selection criteria were applied.

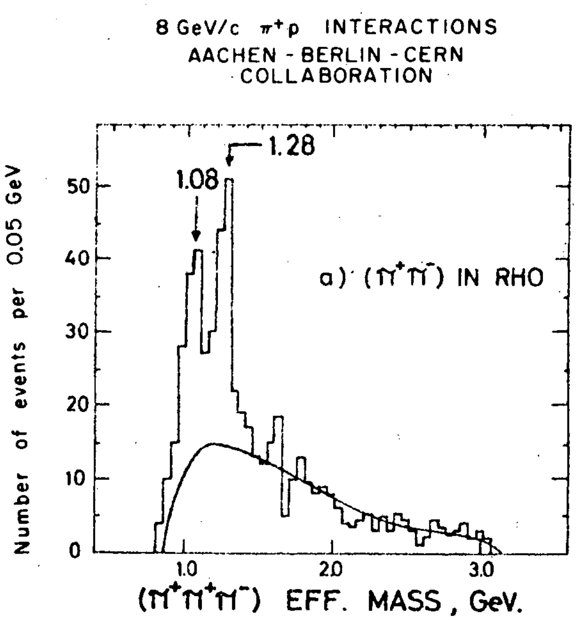

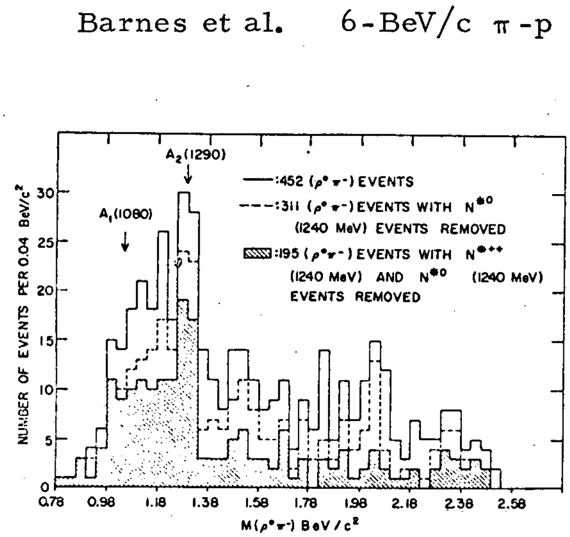

MUB-9790 A

Fig. 4. (left) The $\pi\rho$ mass distribution at 8 BeV/c incident π^+ momentum. This represents the strongest evidence for a sharp A_1 peak. (right) The same distribution from the π^-p interaction at 6 BeV/c. In these data no evidence for the A_1 was observed.

Bozóki et al.

17.2-BeV/c π^- on emulsions

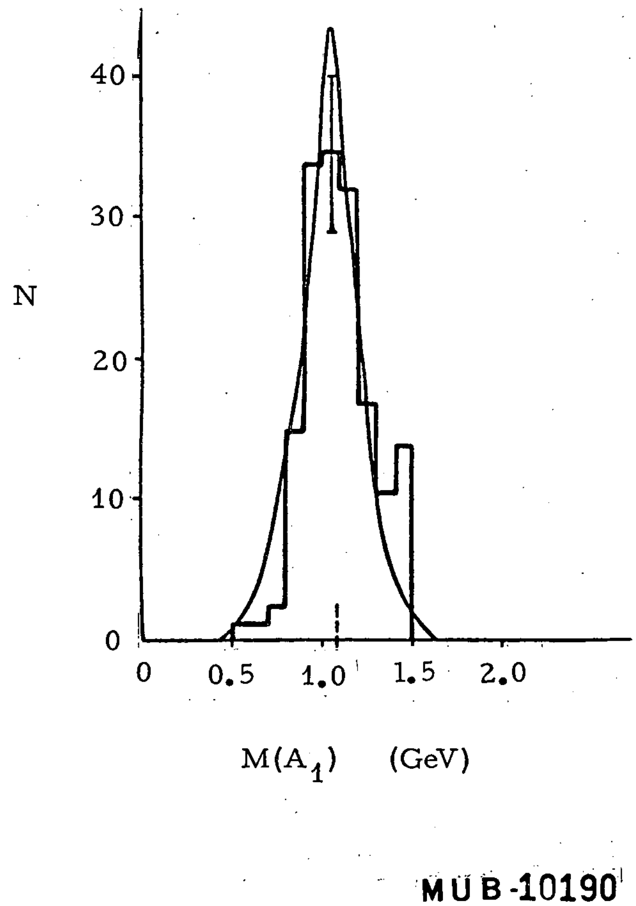

Fig. 5. The distribution of the effective three-pion mass for 142 events. The smooth curve is the effective-mass distribution predicted by the diffraction dissociation mechanism.

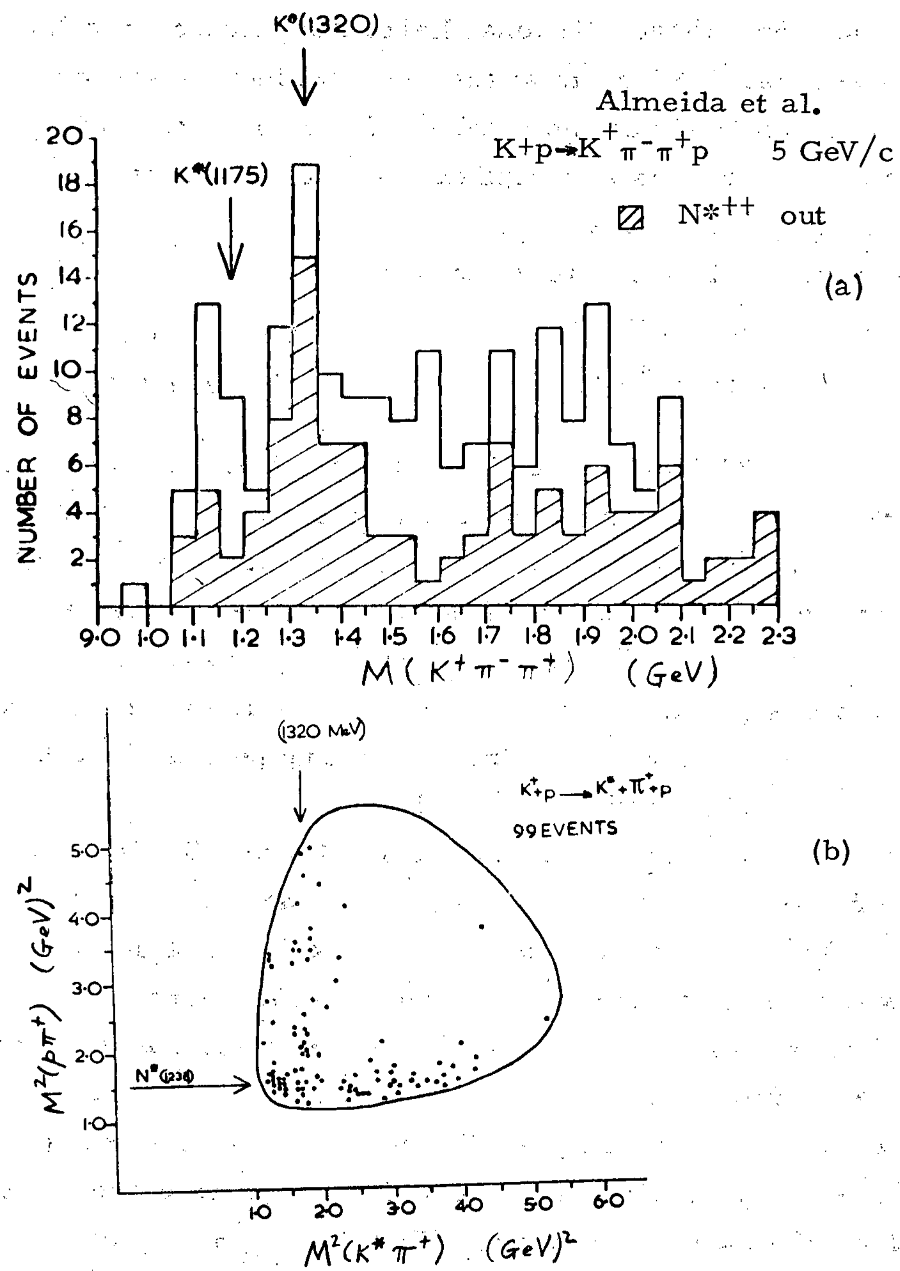

MUB-9792 A

Fig. 6. The initial evidence for the $K^{**}(1320)$.
(a) The $K^+\pi^-\pi^+$ mass distribution without K^* selection.
(b) The Dalitz plots for the $K^*\pi^+p$ events.

In our own work[11] with $K^+ + p$ at 4.6 BeV/c, obtained from a run with the 80-inch Brookhaven National Laboratory hydrogen bubble chamber exposed in a separated K^+ beam at the AGS, we have observed a very similar effect based on 10 times the number of events, viz., 421 events after the same selection criteria are applied. (These data were first presented at the 1965 Oxford Conference).

We have studied the two reactions

$$K^+ + p \rightarrow K^+ \pi^- \pi^+ p \qquad (997 \text{ events}), \qquad (1)$$

$$\rightarrow K^0 \pi^0 \pi^+ p \qquad (454 \text{ events}). \qquad (2)$$

In (1) $K^{*0}(890)$ is produced, while in (2) both $K^{*0}(890)$ and $K^{*+}(890)$ are produced. Figure 7 gives the triangle plot for Reaction (1). Figure 8a and b shows the corresponding Dalitz plots for Reactions (1) and (2). Here for Reaction (2) both versions of $K^*(890)$ are chosen. The projections in Fig. 8 show the $[K^*(890)\pi]^+$ mass squared and mass distributions for Reactions (1) and (2) separately as well as the combined mass distribution. We observe a very distinct and sharp peak at 1320 MeV with $\Gamma \approx 80$ MeV in both Reactions (1) and (2).

Jongejans also presented data at the Oxford Conference from K^+p at 3, 3.5, and 5 BeV/c (De Baere et al.[12]). The numbers of events for Reaction (1) after applying the above two selection criteria were 102, 130, and 214 respectively, for the three momenta. De Baere et al. concluded from their data that the $K^{**}(1320)$ must be a kinematic effect, because they found that the location of the center of the peak moves as the K^+ incident momentum changes. From Fig. 9, the central masses of the observed peaks (as read off by us) for the three incident momenta are ≈ 1225, ≈ 1350, and ≈ 1225 MeV respectively.[13] The variation they observe does not appear to show a consistent trend and could thus be in part statistical. Although these data certainly favor the kinematical interpretation, we feel that it is not fully conclusive just on this evidence alone. For example, it is conceivable that the $K^{**}(1320)$ gets produced only above 3.5 BeV/c incident momentum. We thus feel that more data will be needed to settle this point.

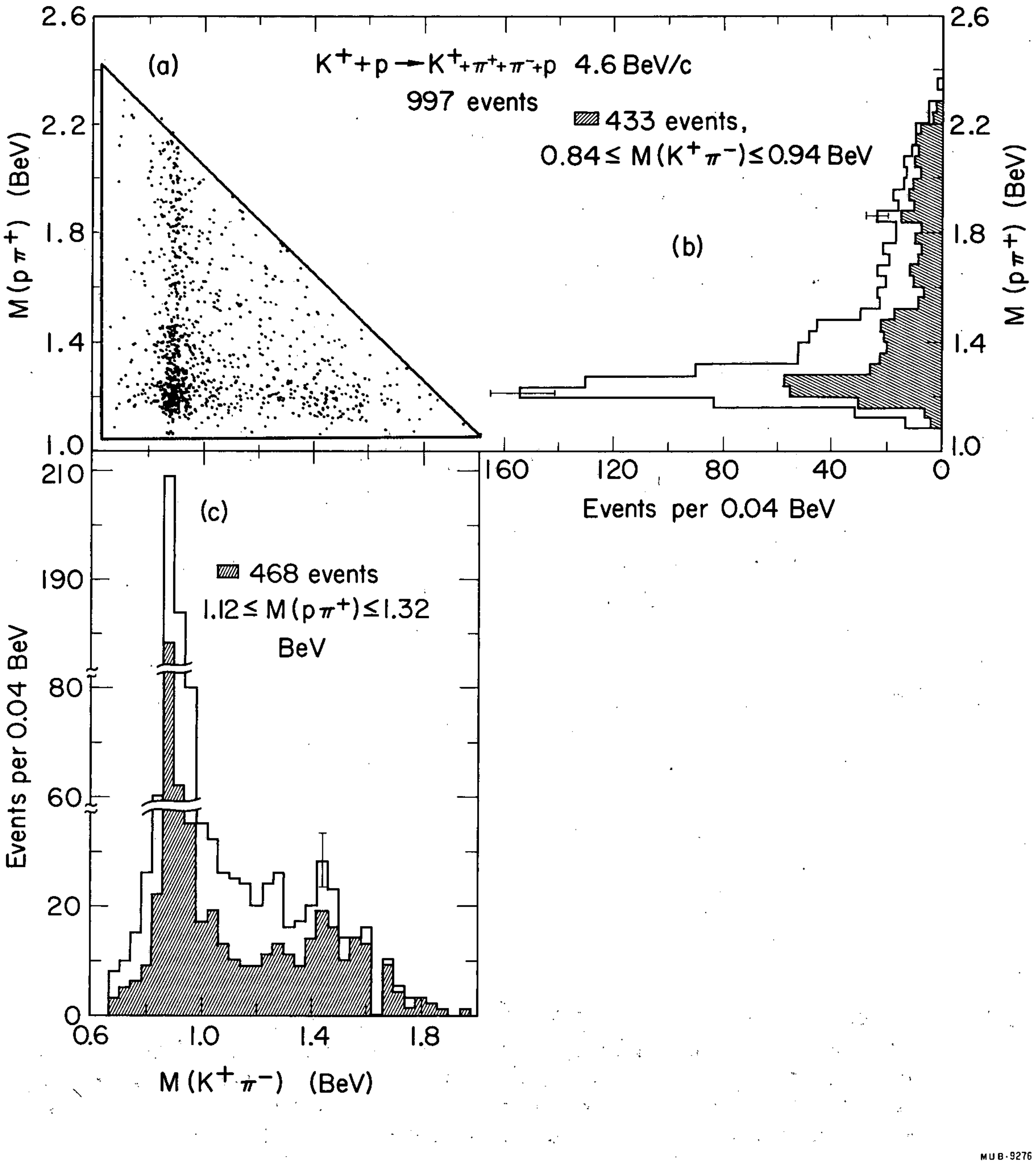

Fig. 7. In the triangle plot for the reaction $K^+ + p \to K^+ + \pi^+ + \pi^- + p$ at 4.6 BeV/c, the $K^{**}(1320)$ phenomenon corresponds to the $K^*(890)$ events found in the vertical band outside the N^{*++} horizontal band.

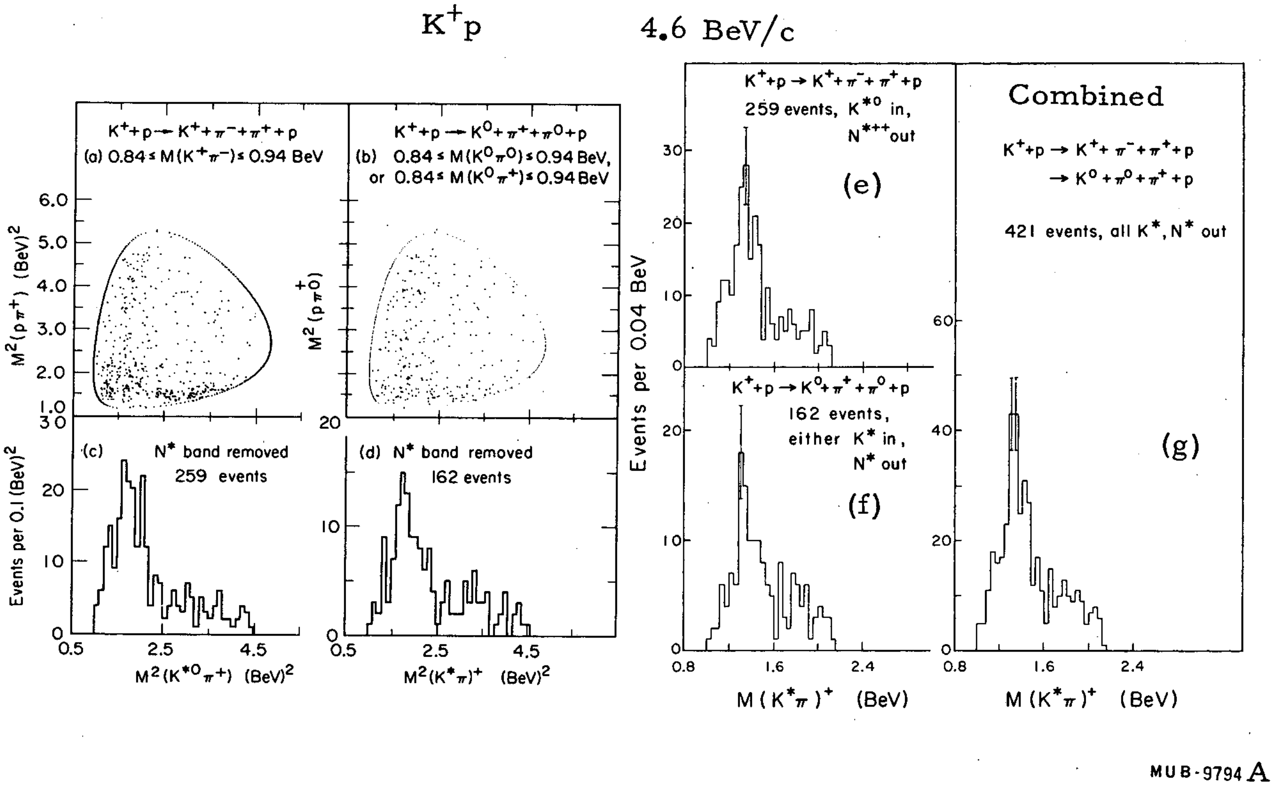

Fig. 8. The Dalitz plots for the $K^*\pi p$ events. The projections are shown in (c) and (d) in mass squared and in (e) and (f) in mass. The combined distribution is shown in (g). The latter shows the mass peak in the $K^*\pi$ mass distribution at 1320 MeV/c and a possible indication of an enhancement at 1400 MeV/c.

De Baere et al.

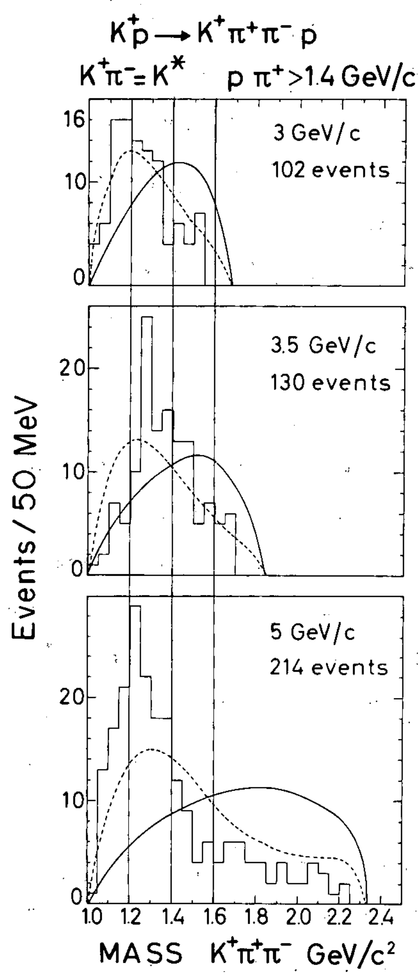

Bishop et al. 3.6-GeV/c K^+p

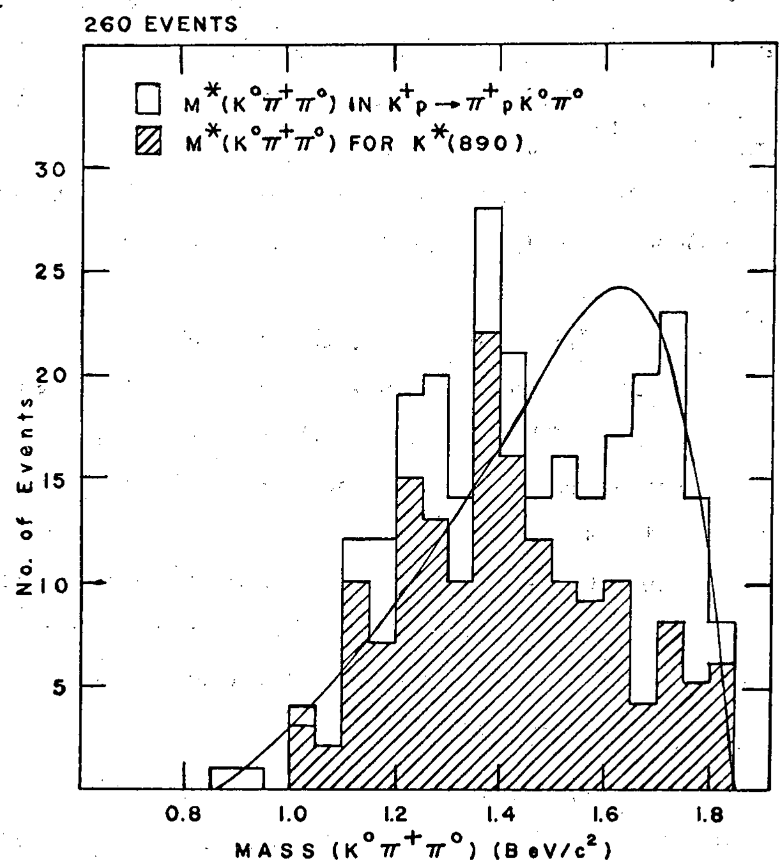

MUB-9881A

Fig. 9. (left) The same mass distribution as in Fig. 8 from the experiment of De Baere et al.

Fig. 10. (right) The same distribution as in Fig. 8 from the data of Bishop et al.; the shaded region corresponds to $K^*(890)$ selection. In these data the N^{*++} has not been removed. The authors point out the small enhancement at 1400 MeV/c.

One amusing feature is that not only does the 1320-MeV $K^* \pi$ peak correspond to the A_1, but there is also the possibility of a second peak due to the $K^*(1400)$ decay via $K^*(890) + \pi$, which would correspond to the A_2. Thus here again we would have a situation in which we observe an SU(3) analog (this time from the 2^+ nonet). The very persuasive arguments of Glashow and Socolow[14] on the 2^+ nonet predict $[K^*(1400) \to K^*(890)\,\pi]/[K^*(1400) \to K\pi] = 0.6$. Although we observe a small peak in the $K^*(890)\,\pi$ mass distribution in the region of 1400 MeV (see Fig. 8), our present data do not allow us to give a significant determination of this ratio. Bishop et al.[15] have shown some evidence for this decay mode in their experiment with 3.6-BeV/c K^+p (see Fig. 10), while Chung et al.[16] quote a limit for this decay mode. Furthermore, Derrick also presented evidence for this decay mode, based on the K^-p interactions at 5.5 BeV/c, at the 1966 New York Meeting.[17]

III. KINEMATIC ENHANCEMENT MECHANISMS

Even before its discovery, the A_1 was predicted as a kinematic enhancement. Thus Pais and Nauenberg[18] predicted a peak in the $\pi\rho$ mass at the position of the A_1 on the basis of the Peierls mechanism.[19] However, more careful study of this phenomenon, in particular by Goebel,[20] indicates that the Peierls mechanism cannot give rise to such a peak, at a physical mass value. New mechanisms have been suggested more recently, again considering the A_1 as a kinematic enhancement.

A. The Deck Mechanism

In Deck's model,[21] and the further elaboration by Maor and O'Halloran,[22] it was shown that the qualitative features of a peak in the $\pi\rho$ mass near the A_1 can be obtained from an OPE calculation in which the lone pion scatters off the nucleon. (These models differ in detail in that Deck, in the spirit of the Drell process, has considered the πp scattering vertex purely as diffraction scattering. Maor and O'Halloran, on the other hand, have considered the physical πp cross sections with off-the-mass-shell corrections. At the higher πp mass values these two approaches differ only slightly.) Figure 11, gives the result of the calculations by Maor

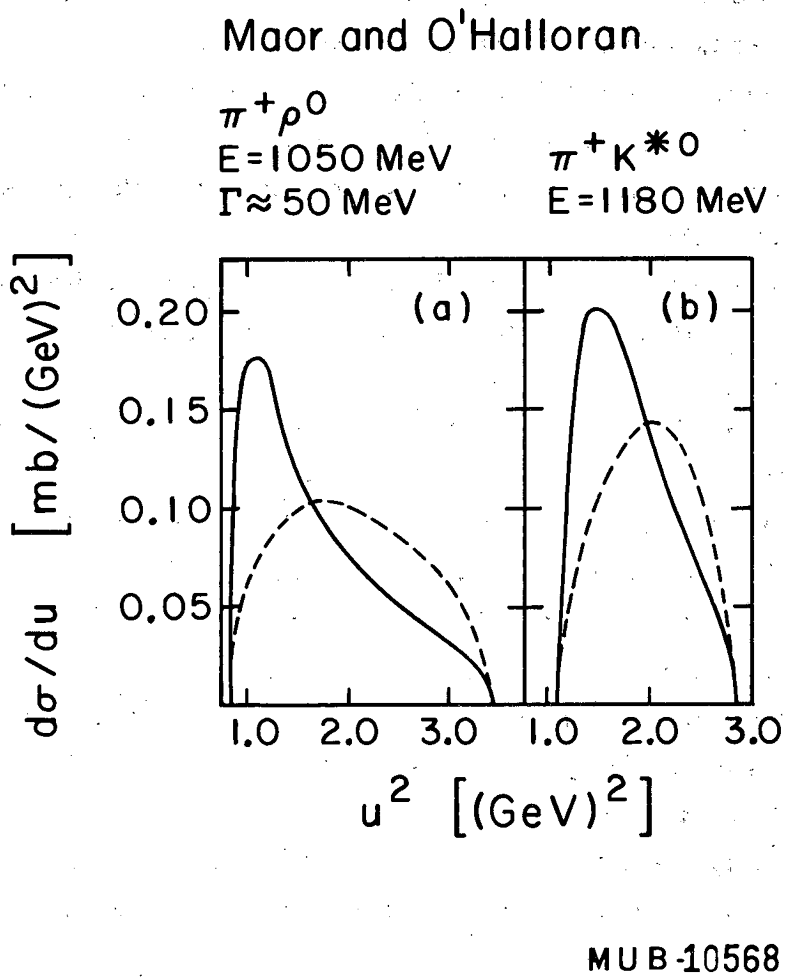

Fig. 11. (a) π^+-ρ^0 calculated mass distribution for 3.6 GeV/c incident momentum. (b) π^+-K^{*0} calculated mass distribution at 3.0 GeV/c. Calculations based on asymmetry of π^+p scattering above N^{*++} resonance. Both distributions are compared with the appropriate normalized phase-space distributions (dashed lines).

and O'Halloran.

A word of caution. We feel sure that the above authors will agree with us that the exact shape, location of peak, and width of peak must be considered only as qualitative indications from their calculations. In particular, such questions as absorption effects versus form factors and the exact handling of spin >3/2 resonances have not been settled as yet. Furthermore, Bose symmetrization effects have not been included in the calculations either.

If we take this model, involving virtual pion exchange, seriously, it carries with it some further specific conditions, which can be tested.

We can state these as follows:

(a) The ρ^0 should be produced aligned with respect to the incident direction, such that the $\pi\pi$ scattering angle $\alpha_{\pi\pi}$ in the ρ^0 center of mass follows the distribution $\cos^2 \alpha_{\pi\pi}$.

(b) The Treiman-Yang angle at the ρ^0 vertex should be isotropic (except perhaps for small deviations due to absorption effects).

(c) The Treiman-Yang angle at the πp vertex also should be isotropic (with a similar proviso for possible absorption effects).

(d) The four-momentum transfer distribution to the ρ^0 meson should be "characteristic of the OPE model."

(e) The differential cross section $d^2\sigma/d\Omega dM$ of the $\pi^\pm p$ vertex should be similar to that for free $\pi^\pm p$ elastic scattering, $\langle d\sigma_{el}/d\Omega \rangle$, when averaged over the corresponding mass interval.

In the above discussion we have made all statements in terms of A_1 production. They are equally applicable to $K^{**}(1320)$ production, in which the ρ^0 is replaced by the $K^*(890)$.

With respect to points (a) through (d) we have two control regions we can consider for the A_1 (which is here assumed to be a kinematical enhancement). First we can compare the angular and four-momentum distributions obtained for the A_1 band with distributions corresponding to $\rho^0 N^{*++}(1238)$ production. Here we have a control region and expect to see similarities in the distributions, since the N^{*++} is just part of the $\pi^+ p$ scattering cross section, albeit a very intense and well-defined part. Secondly, we can contrast the distributions in the A_1 band with those in the A_2 band. Here we expect to see radical differences, as the events in the A_2 band (aside from background) definitely correspond to a bona fide resonance with $J^P = 2^+$.

Furthermore even if A_1 is a meson (of spin-parity $J^P \neq 2^+$) we do not expect the same angular distributions. However, one might have expected comparable $\Delta^2(\rho)$ distributions (both corresponding to ρ exchange); but these are observed to be distinctly different. One further point of interest is the lack of asymmetry in ρ^0 decay (the cos $\alpha_{\pi\pi}$ distribution) in the A_2 band, while the usual asymmetry is present for the A_1 band (see Sections IV E and H).

For the $K^{**}(1320)$ we have only the $K^*(890) + N^{*++}$ events as control region, where we must again look for similarities. [As pointed out above, the $K^*(1400) \to K^*(890) + \pi$ decay mode is not pronounced enough in our data to be useful as a region of comparison in analogy to the A_2].

B. Other Mechanisms

Other kinematic mechanisms have been proposed to explain the A_1 enhancement as well. Month[23] proposed triangle singularities as a source for the enhancement, and Chang,[24] and Dash et al.[25] considered enhancements arising from Bose symmetrization effects. These mechanisms do not possess such well-defined tests as points (a) through (e) above, that can be performed with the data; we will not pursue these further here. (Month's proposal would require considerable low-mass $\pi\pi$ enhancement for the A_1, and $\pi\pi$ and/or $K\pi$ enhancement or both for $K^{**}(1320)$. No effects strong enough to produce the observed phenomenon are seen in either case. See Fig. 32 for the A_1 case.)

IV. THE EXPERIMENTAL RESULTS AND TESTS ON THE A_1 PERTAINING TO KINEMATIC ENHANCEMENT

A. Results from the British-German collaboration

In this work (π^+p at 4 BeV/c) Aderholz et al.[26] compared the experimental data with an OPE calculation similar to the Deck model. They studied the $\pi\rho$ mass distribution (see Fig. 12a), the $\alpha_{\pi\pi}$ scattering angle in the ρ^0 center-of-mass system, see Fig. 12b and c, and the Δ^2 distribution to the $\pi\rho$ system, Fig. 12d and c. In the latter two the A_2 band is used as a control region for the A_1, and marked differences are noted. They conclude that the general features of the events in the A_1 region are described by the OPE model except for the height and narrow width of the A_1 enhancement. They thus felt that they could not decide between "meson" and "kinematic enhancement."

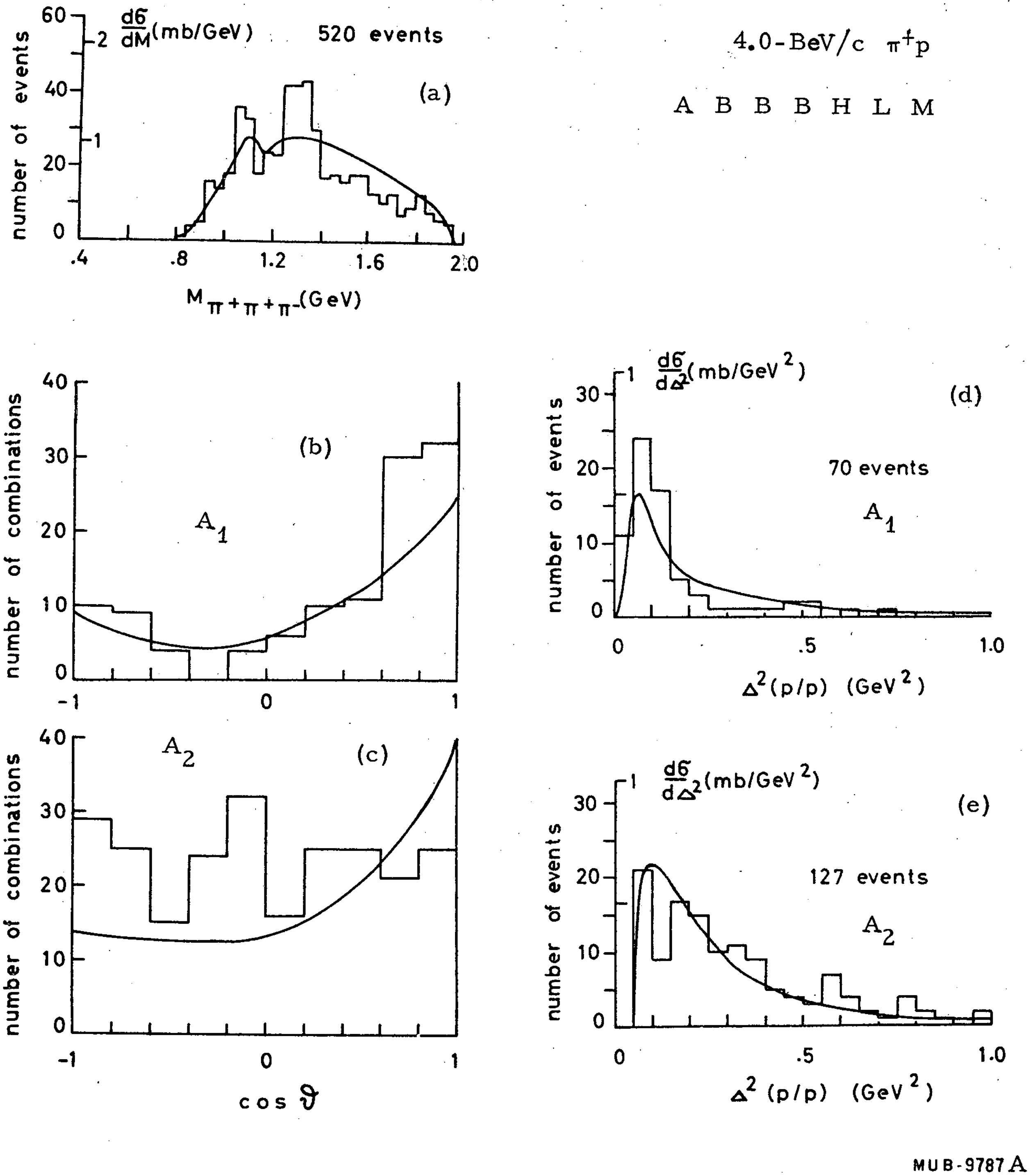

Fig. 12. The data from the 4-BeV/c π^+p experiment; (b) and (c) show the distribution of the $\pi\pi$ scattering angle in the ρ^0 center of mass. This was called $\alpha_{\pi\pi}$ in the text.

B. The work on the $\pi^- d$ interaction

The $\pi^- d$ reaction studied by Seidlitz et al.[27] at 3.2 BeV/c and by Abolins et al.[28] at 3.7 BeV/c, allows one to rule out the isotopic spin T = 2 for both the A_1 and A_2. The argument rests on the comparison of the production rates for the A_1 and A_2 in the reactions

$$\pi^- d \rightarrow \rho^0 + \pi^- + n + (p); \quad \rho^0 \rightarrow \pi^+\pi^- \qquad (1a)$$

or

$$\rightarrow \rho^0 + \pi^- + p + (n); \quad \rho^0 \rightarrow \pi^+\pi^- \qquad (1b)$$

and

$$\pi^- + d \rightarrow \rho^- + \pi^- + p + (p); \quad \rho^- \rightarrow \pi^-\pi^0; \qquad (2)$$

thus they search for the rates of $A^- \rightarrow \rho^0 + \pi^-$ from Reactions (1a) and (1b) and $A^{--} \rightarrow \rho^- + \pi^-$ from Reaction (2), which should be 1:1:0 for T(A) = 1 and 1:1:8 for T(A) = 2. The data show clearly (Figs. 13 and 14) that both A_1 and A_2 correspond to T = 1 effects. Seidlitz et al. stress in particular that the events in the A_1 region are associated with very small Δ^2 to the $A_1[\Delta^2(\pi^-\rho^0) \leq .15\ (\mathrm{BeV/c})^2]$, which appears inconsistent with the interpretation of the A_1 as a resonance in $\pi\rho$ scattering (and thus corresponding to ρ exchange). They cite the work of Cohn et al.,[29] who observed ω production in the reaction $\pi^+ + d \rightarrow \omega + p\ (p)$ at 3.65 BeV/c (assumed to proceed via ρ exchange). Cohn et al. find that no appreciable amount of ω production occurs for $\Delta^2\ (\omega) \leq 0.6(\mathrm{BeV/c})^2$, which is also the case for A_2 production.

C. The comments by Xuong

In his talk at the 2nd Athens Conference Ng. H. Xuong, reporting on the data of Abolins et al.,[28] made two further comments about the A_1 phenomenon.

(a) He showed that in the reaction $\pi^+ p \rightarrow \pi^+\pi^-\pi^+ p$ one can use the events corresponding to a $\rho^0 N^{*++}$ formation to produce a "pseudo Deck effect." By studying the $\rho^0\pi^+$ mass distribution for these events he showed that a peak in this mass distribution near the A_1 can be obtained by choosing the events corresponding to the forward decay of the N^{*++} (see Fig. 15). Thus he achieved by artificial means what the diffraction effect does "naturally" at πp masses above the N^* band. While this strengthens the Deck model, he points out that it does not prove that the A_1 is not a meson.

Seidlitz et al. 3.2-BeV/c π^-d

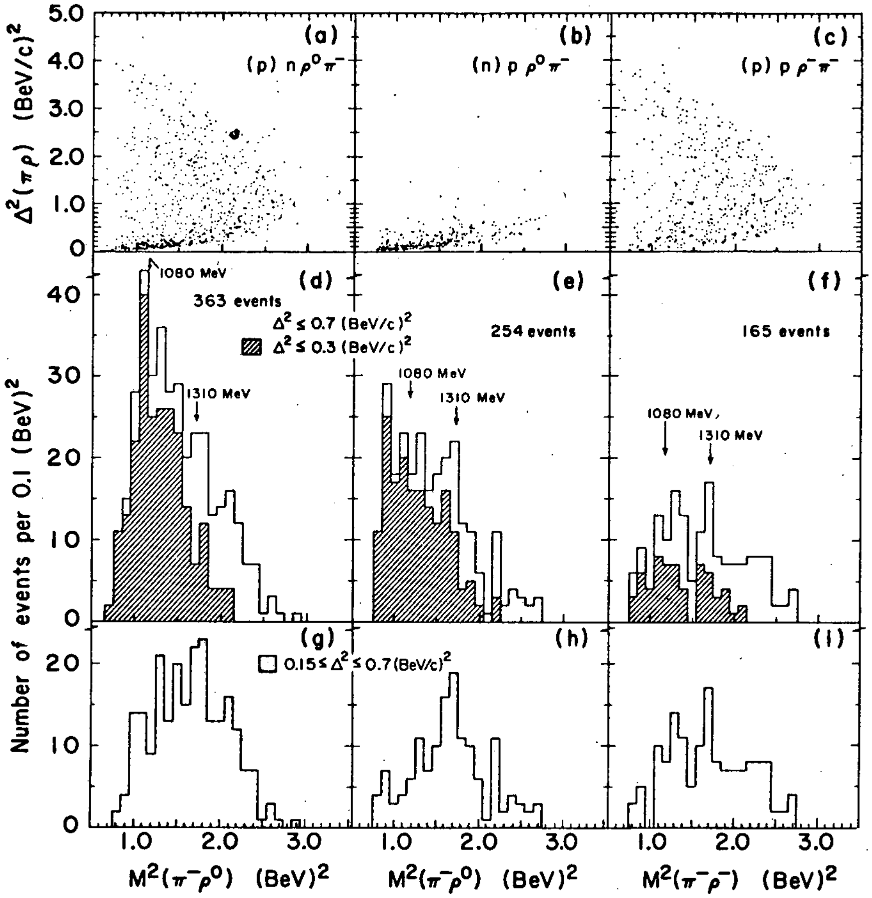

MUB-9789A

Fig. 13. (a), (b), and (c): Chew-Low plots of the $\pi\rho$ systems in the reactions indicated. (d) through (i): Projections of mass squared (πp) for the same reactions. In all plots, events were excluded if neither $\pi^{+,0}\pi^-$ pair was in the ρ interval (600 to 850 MeV). Events with either $n\pi^-$ pair (a), the $p\pi^+$ pair (b), or either $p\pi^-$ pair (c) in the N^* interval (1120 to 1320 MeV) were excluded.

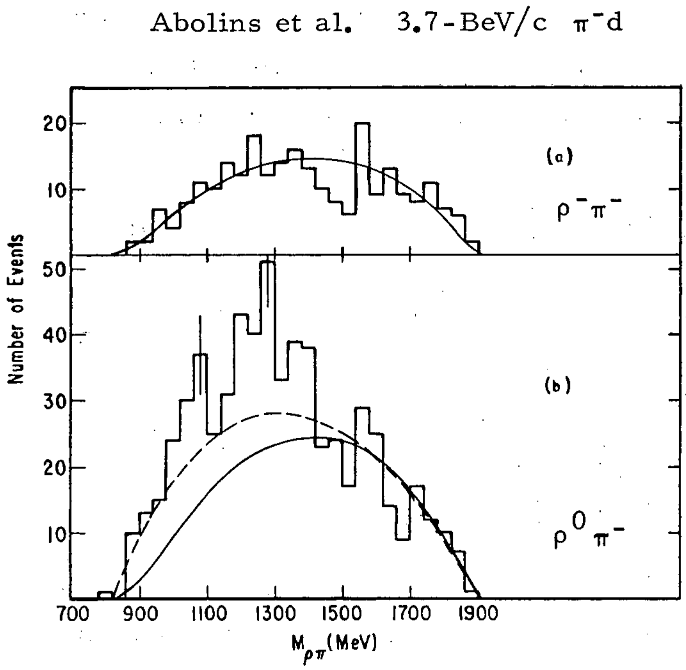

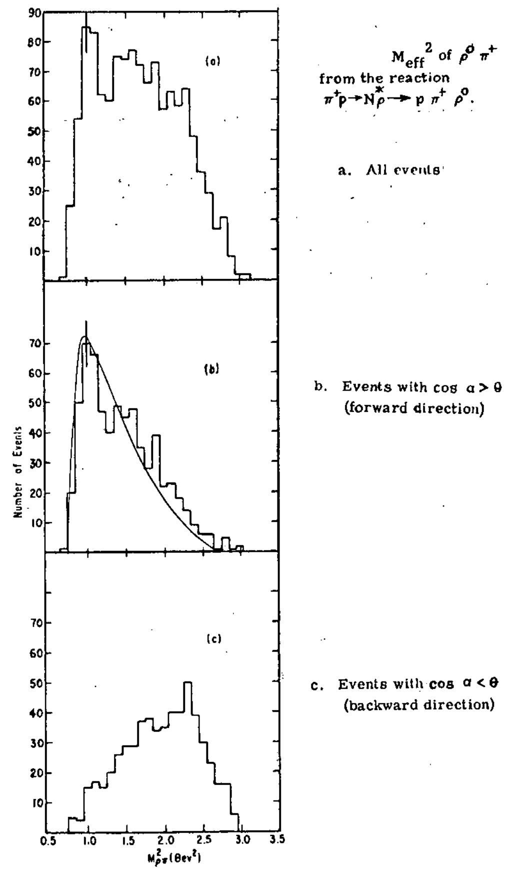

MUB-9791 A

Fig. 14. (left)(a) Effective-mass distribution of the $\rho^-\pi^-$ combination from reaction $\pi^- d \rightarrow pp\rho^-\pi^- \rightarrow pp\pi^-\pi^0\pi^-$.
(b) Effective-mass distribution of the $\rho^0\pi^-$ combination from reaction $\pi^- d \rightarrow pn\rho^0\pi^- \rightarrow pn\pi^-\pi^0\pi^-$.
Solid curves are phase-space estimates. Broken line is a smooth curve normalized to fit the region outside the A_1 and A_2 masses.

Fig. 15. (right) M_{eff}^2 of $\rho^0\pi^+$ from the reaction $\pi^+ p \rightarrow N^*\rho \rightarrow p\pi^+\rho^0$.
(a) All events (b) Events with $\cos\alpha > \theta$ (forward direction).
(c) Events with $\cos\alpha < \theta$ (backward direction).

(b) He suggests an additional test for the A_1 phenomenon. In the reaction $\pi^+ + p \rightarrow N^{*++} + \rho^{+,0,-} + \pi^{-,0,+}$, the decay $A_1 \rightarrow \rho^0 + \pi^0$ is forbidden for a $T = 1$ meson (Clebsch-Gordan Coefficient = 0) and allowed in the Deck Model. While $A_1 \rightarrow \rho^- + \pi^+$ is "forbidden" in the Deck model (exchange of a doubly charged object would be required), it is allowed for a $T = 1$ meson. This test may, however, be rather academic, as at the energies investigated so far no appreciable A_1 peak has been observed in the above reaction.

D. <u>A similar test proposed by Kirz</u>

A very similar proposal was made by Janos Kirz.* He suggested the study of the reaction

$$\pi^+ d \rightarrow ppA_1^0. \tag{3}$$

Here, again if A_1 is a meson,

$$A_1^0 \rightarrow \rho^- + \pi^+, \tag{4}$$
$$\rightarrow \rho^+ + \pi^-, \tag{5}$$
$$\not\rightarrow \rho^0 + \pi^0. \tag{6}$$

This reaction has the virtue that it can be quantitatively compared (from I-spin considerations) with the reactions

$$\pi^\pm p \rightarrow p + A_1^\pm$$
$$\hookrightarrow \rho^0 + \pi^\pm. \tag{7}$$

Thus Reaction (3) followed by the decay mode (4) or (5) should be in the ratio 2:1 with reactions (7), while decay mode (6) is forbidden. On the other hand, on the Deck model, (3) followed by (4) is forbidden; all other reactions are allowed and semiquantitative ratios can be obtained for them based on the appropriate πp scattering cross sections. If this test is performed at energies at which Reaction (7) gives a clear-cut A_1 peak--e.g., for 8-BeV/c π^+ mesons (if we accept the present data at face value)--it should result in a conclusive answer on the A_1 phenomenon.

---

*This proposal is quoted by A. H. Rosenfeld, Ref. 13.

E. The approach by Shen et al.

In our own work with π^+p at 3.65 BeV/c and π^-p at 3.7 BeV/c (Shen et al.[30]) we considered the events with ρ^0 production, $\pi^\pm p \rightarrow \rho^0 \pi^\pm p$. We then asked ourselves the question whether, aside from any considerations on A_1 and A_2 production, we observe the Drell process,[31] i.e., scattering of the virtual pion from the proton. We answered this question in the affirmative based on the following arguments:

Let us consider the proton vertex in the Feynman diagram shown in Fig. 16. Here we can look at the correlation between the $\pi^\pm p$ mass for the outgoing particles and the p_{in}, p_{out} scattering angle α_{pp} in the $\pi^\pm p$ rest system. This is shown in Fig. 16a and c. We note two distinct features: (a) an enhancement of events in the region of the 3/2, 3/2 resonances N^{*++} (1238) and N^{*0} (1238), the latter at about 10% the intensity of the former; (b) a very strong enhancement of events at small scattering angles, $\cos\alpha_{pp} \geq 0.8$, for both the π^+p and π^-p data. As may be noted from Fig. 16, the $\cos\alpha_{pp}$ distribution becomes more forward peaked with increasing mass of the outgoing $\pi^\pm p$ system, $M(\pi^\pm p)$, in a manner characteristic of diffraction scattering. Figure 17a and b shows the same correlation in three-dimensional plots. To further investigate this effect we have divided the $\pi^\pm p$ mass distribution into four intervals of width 0.25 BeV, starting at 1.09 BeV. These intervals were chosen so that the corresponding differential cross sections represent averages over the various known N^* resonances. Thus the first interval includes the $N^*_{3/2}$ (1238) resonances. The next two intervals encompass various resonances near 1500 and 1700 MeV in the π^-p system. The last interval, 1.84 to 2.09 BeV, includes the $N^*_{3/2}$ (1920) resonance. The differential cross sections for the first three energy bands are given in Fig. 18 for a Δ^2 cutoff to the $\pi^\pm p$ system of $1.0(\text{BeV}/c)^2$. It is important to note that this has the effect of virtually eliminating the contributions from the A_2 meson (see Fig. 22 below). The corresponding $\pi^\pm p$ mass projections are shown shaded in Fig. 16b and d. For the mass interval 1.84 to 2.09 BeV our small sample of events did not permit us to eliminate events with $\Delta^2_{\pi^\pm p} > 1\ (\text{BeV}/c)^2$. In order to investigate this mass region as well we have chosen to remove events associated with the A_2 band ($1.26 < M_{\pi^\pm\rho^0} < 1.38$ BeV).

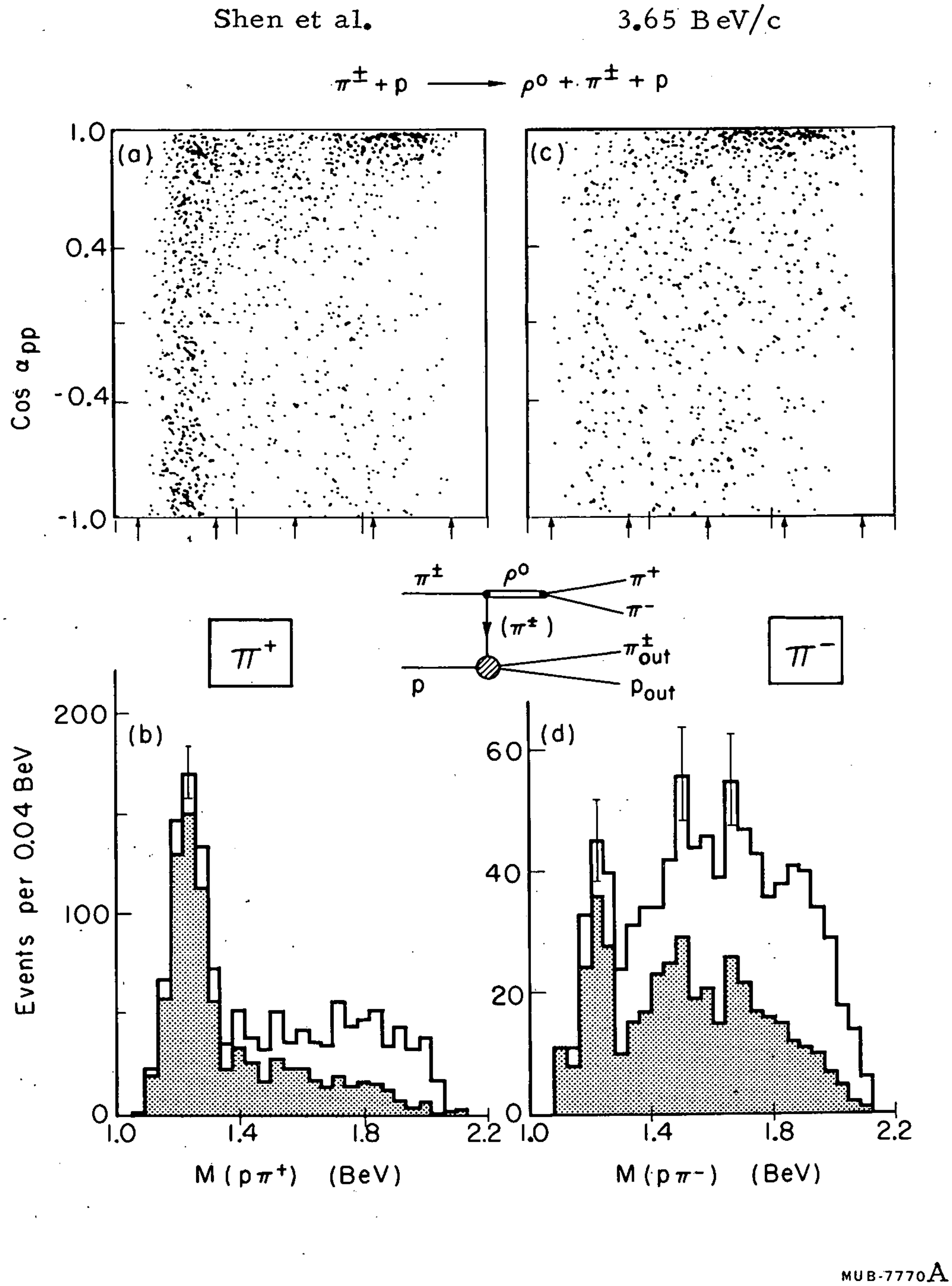

Fig. 16. Scatter plots of $\cos \alpha_{pp}$ versus $M(p\pi^{\pm})$ for $\pi^{+}p$ and $\pi^{-}p$ interactions. The mass projections are shown in (b) and (d) respectively. The shaded regions correspond to $\Delta^{2}(p\pi^{\pm}) \leq 1.0$ $(BeV/c)^{2}$. The arrows delineate the four mass regions discussed in the text.

Shen et al. 3.65 BeV/c

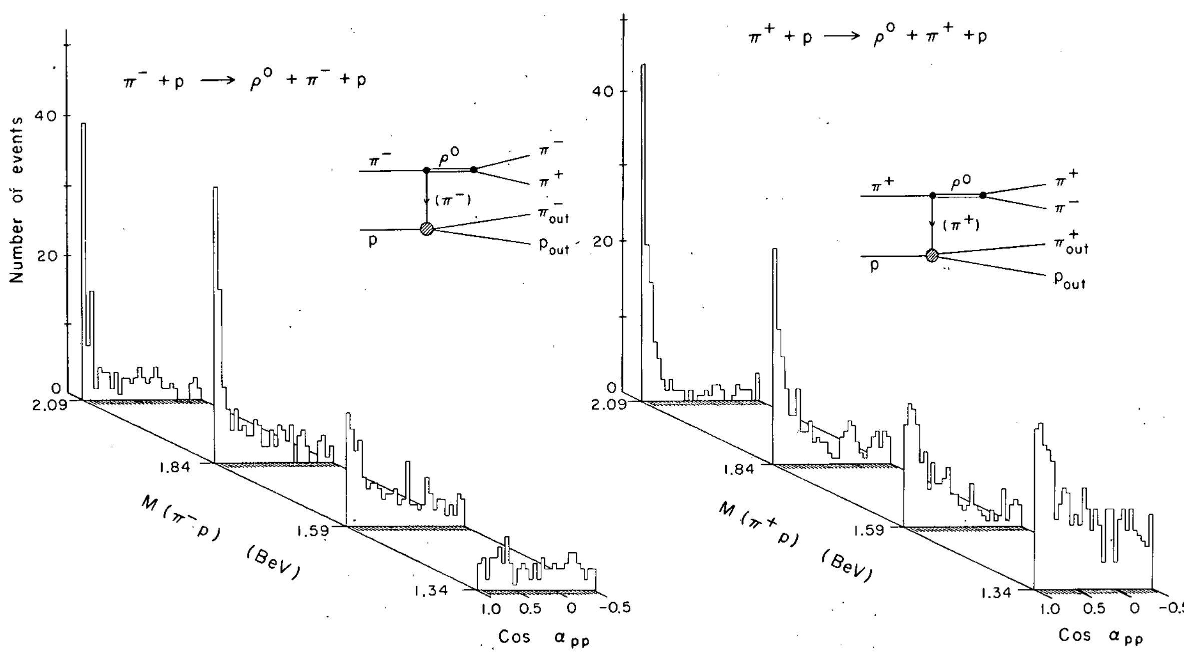

Fig. 17. Three-dimensional plots of the mass in the π^-p and π^+p system respectively versus cos α_{pp}. This shows how the angular distribution sharpens up in the forward direction as the $\pi^{\pm}p$ mass increases. [Technical note: these plots were drawn automatically from the computer output.]

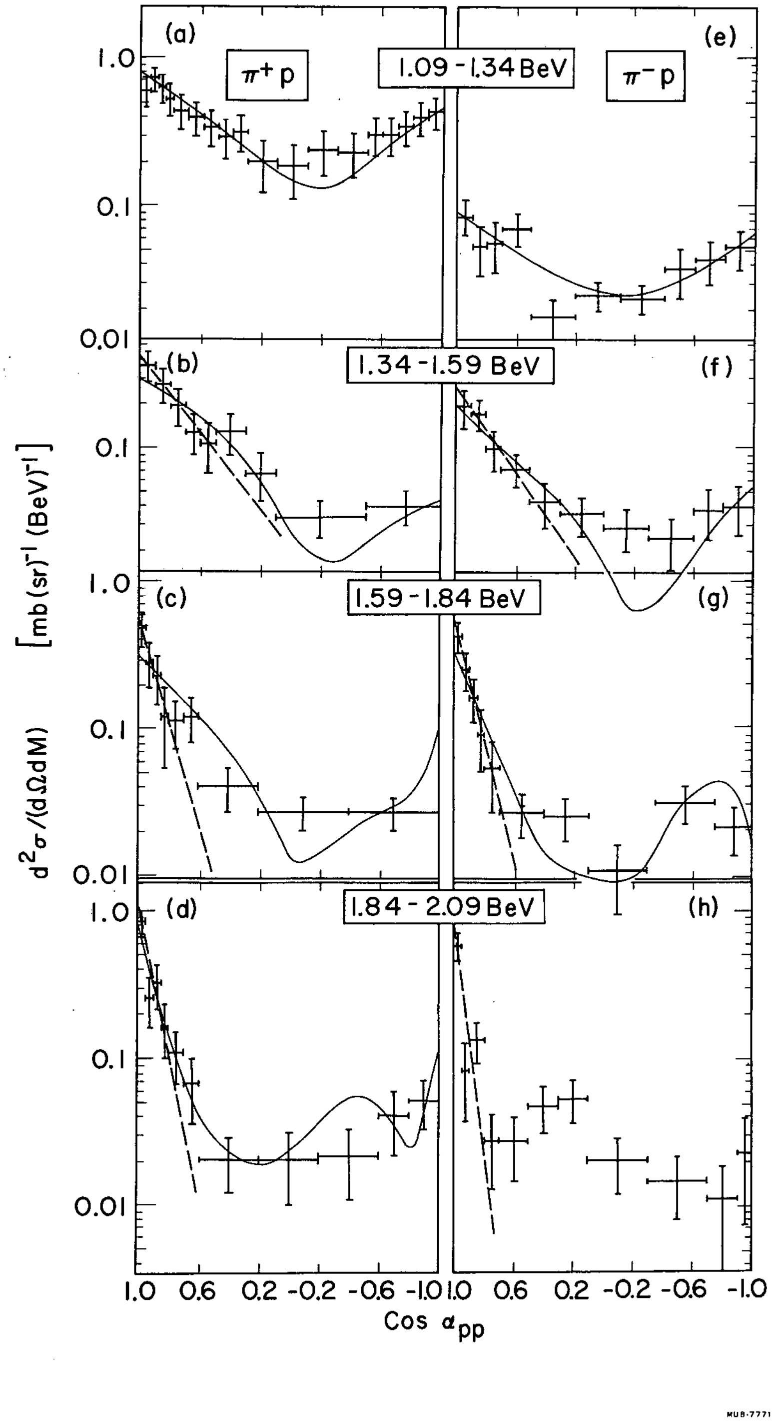

Fig. 18. Data of Shen et al. The differential cross section $d^2\sigma/(d\Omega dM)$ for the four $M(p\pi^\pm)$ regions. Parts (a), (b), (c) and (e), (f), (g) correspond to $\Delta^2(p\pi^\pm) \leq 1.0\ (BeV)^2$. In parts (d) and (h) no Δ^2 cut-off is applied. The A_2 band is removed, however. The curves correspond to elastic $\pi^\pm p$ scattering cross sections averaged and normalized as discussed in the text. The dotted lines illustrate the exponential dropoff at small angles.

We have taken two distinct approaches in parameterizing these experimental data, as follows.

a. Diffraction scattering at the $\pi^{\pm}p$ vertex

We find that the data at small α_{pp} values can be represented by the same variation with t, namely e^{-at}, which holds for $\pi^{+}p$ and $\pi^{-}p$ scattering on the mass shell. We find that the a_{+} and a_{-} values for "virtual" $\pi^{+}p$ and $\pi^{-}p$ scattering lie in the region 8 to 12 $(\mathrm{BeV})^{-2}$. The dashed lines on the semilog plots in Fig. 18 indicate that at small angles a good fit can be obtained with an exponential dropoff.

b. Comparison with elastic $\pi^{\pm}p$ scattering experiments

Here we have taken the available experimental $\pi^{+}p$ and $\pi^{-}p$ elastic differential scattering cross sections from counter experiments and have averaged these over the four mass intervals specified above, i.e.,

$$\left\langle \frac{d\sigma_{el}}{d\Omega} \right\rangle = \int_{M_i}^{M_j} \frac{d\sigma_{el}}{d\Omega}\, dM/(M_j - M_i).$$

We have compared these distributions with our experimental $\frac{d^2\sigma}{d\Omega dM}$ distributions by normalizing the elastic differential cross section to the experimental points in the $\cos\alpha_{pp}$ region 0.8 to 1.0. We find that the general shapes of our experimental distribution, although somewhat more peaked near $\alpha_{pp} \approx 0$, are remarkably close to the distributions of $\frac{d\sigma_{el}}{d\Omega}$. We conclude that here, unless one were to ascribe this feature to some accidental effect, we have experimental evidence for point (e) in Section IIIA.

We now turn to the question of the A_1 and A_2 "mesons," which are observed as enhancements in the $\pi^{\pm}\rho^{0}$ system. If we limit ourselves to the sample of events primarily associated with diffraction scattering--i.e., $\cos\alpha_{pp} \geqslant 0.8$ and $M(p\pi^{\pm}) \geqslant 1.34$ BeV--we find a broad enhancement in $M(\pi^{\pm}\rho^{0})$, with evidence of peaking at the A_1 and A_2 bands. Aside from a small A_2 contribution this mass distribution can account for the entire A_1 enhancement observed in our data; see Fig. 19a. On the other hand, eliminating the events associated with diffraction scattering--i.e., $\cos\alpha_{pp} < 0.8$, and leaving the same condition on $M(p\pi^{\pm})$--we remain with a clear A_2 peak (see Fig. 19b), whereas the A_1 peak has completely disappeared.

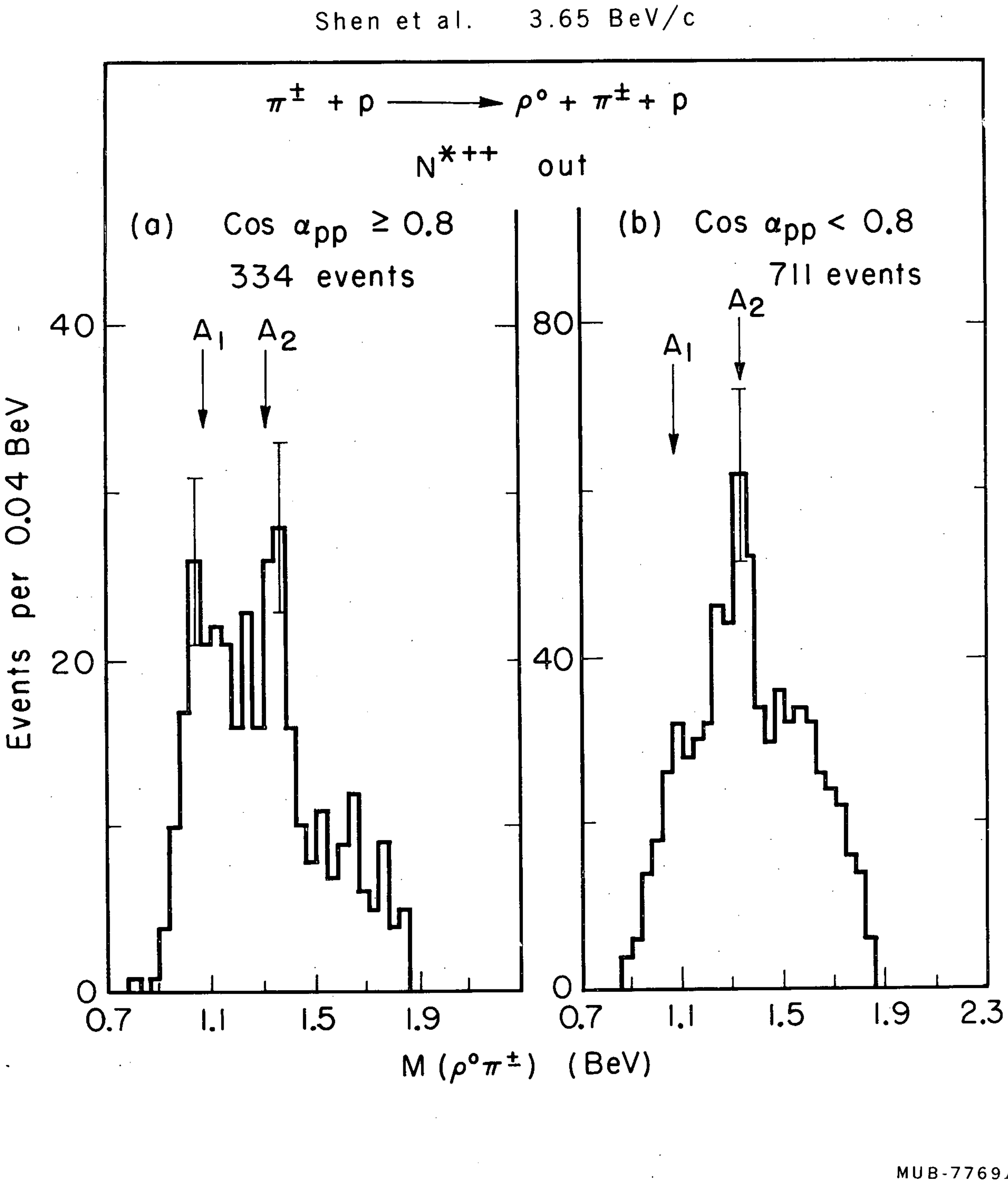

Fig. 19. The $M(\pi^{\pm}\rho^{0})$ mass distribution with the N^{*++} band removed. (a) Distribution for $\cos\alpha_{pp} \geq 0.8$, i.e., for the events we have associated with "diffraction scattering." (b) Events with $\cos\alpha_{pp} \leq 0.8$.

Here we must remark that the condition $\cos\alpha_{pp} > 0.8$ is of course equivalent to small $\Delta^2(A_1)$ values. Thus, although our evidence makes interpretation as a diffraction effect very tempting, it is not the only possible interpretation.

We now turn our attention to points (a) through (d) (in Section IIIA), the alignment of the ρ^0 and the Treiman-Yang angles at the two vertices. These are studied for the A_1 band and the A_2 band as a control region. The results are given in Figs. 20a and b and 21. We note the following:

(a) The ρ^0 is indeed strongly aligned for the A_1 band, although not for the A_2 band (see Fig. 20a).* Another noteworthy feature is that the asymmetry familiar in ρ^0 decay is observed here for the A_1 although not for the A_2 band.

(b) The Treiman-Yang (T-Y) angle at the ρ^0 vertex $\phi(\rho^0)$ is isotropic for the A_1 band; however, it is also essentially isotropic for the A_2 band. It thus follows that the T-Y angle does not appear to be a stringent test in this instance (see Fig. 20b).

(c) The Treiman-Yang angle for the $\pi^{\pm}p$ vertex $\phi(p\pi^{\pm})$ is strongly anisotropic for the A_1 band (see Fig. 21). At first sight this looks bad for the kinematic enhancement model.

There are, however, the following two mitigating factors:

(i) As illustrated in Fig. 21, on introduction of the $\pi^{\pm}\rho^0$ mass cuts (to delineate the A_1 and A_2 bands), the system appears to be overconstrained. That is, as may be noted from Fig. 21, we find a definite correlation between the $\pi^{\pm}\rho^0$ mass cut and the distribution in $\phi(p\pi^{\pm})$. As a further control we have carried out the same $\pi^{\pm}\rho^0$ mass cuts for $\rho^0 N^{*++}$ events, which again show the same correlation. In particular, the $\rho^0 N^{*++}$ events add up to an isotropic distribution (as expected) when all mass cuts are combined to give the "Total" distribution shown in Fig. 21.

---

*This figure differs from the one shown in Ref. 28; the one given here is correct while the one in Ref. 28 includes events in the N^* band as well. There is, however, no qualitative difference between the two, thus all conclusions reached in Ref. 28 remain unaffected.

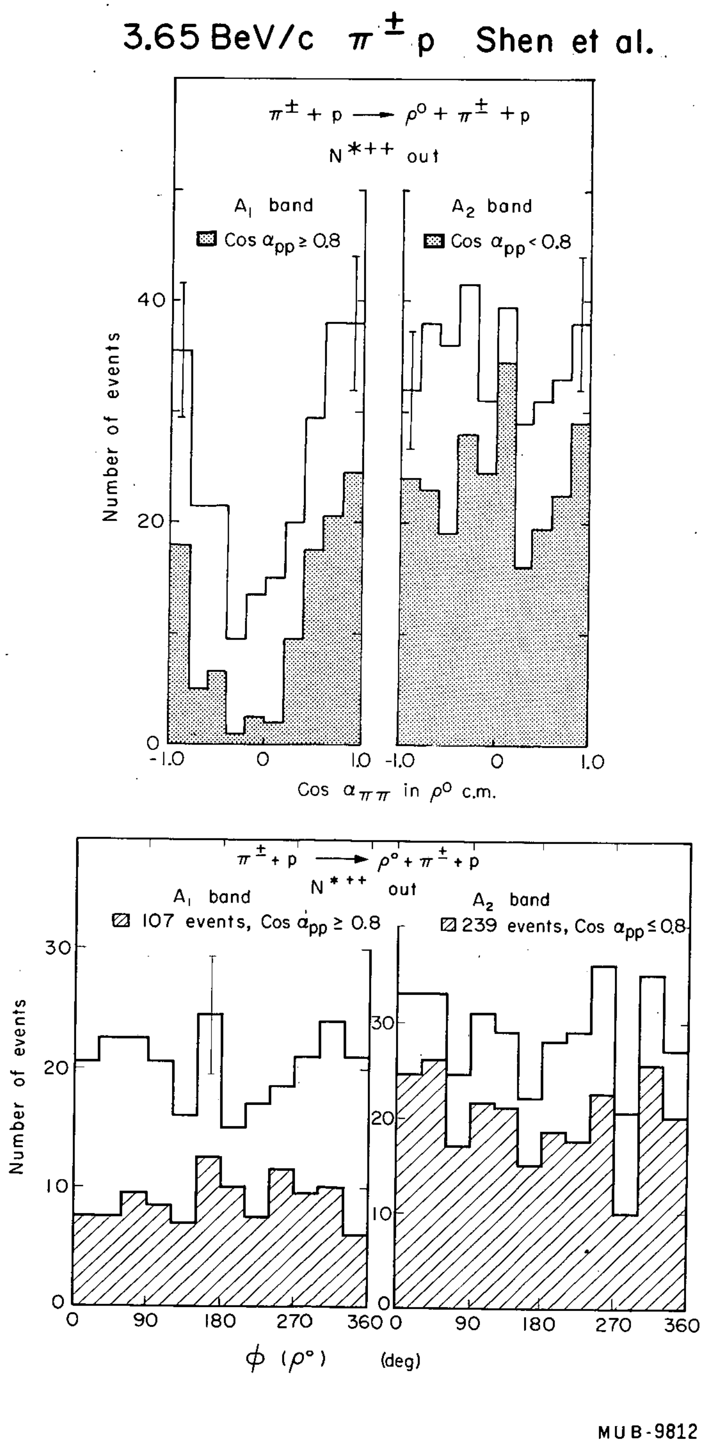

Fig. 20. (upper) Distribution of $\cos\alpha_{\pi\pi}$, the $\pi\pi$ scattering angle in the ρ^0 c.m. The data shown are selected with $\pi^\pm\rho^0$ mass in the A_1 and A_2 bands respectively and for $(\pi^\pm p)_{out}$ masses above the $N^*(1238)$ band. (lower) The corresponding Treiman-Yang angular distribution.

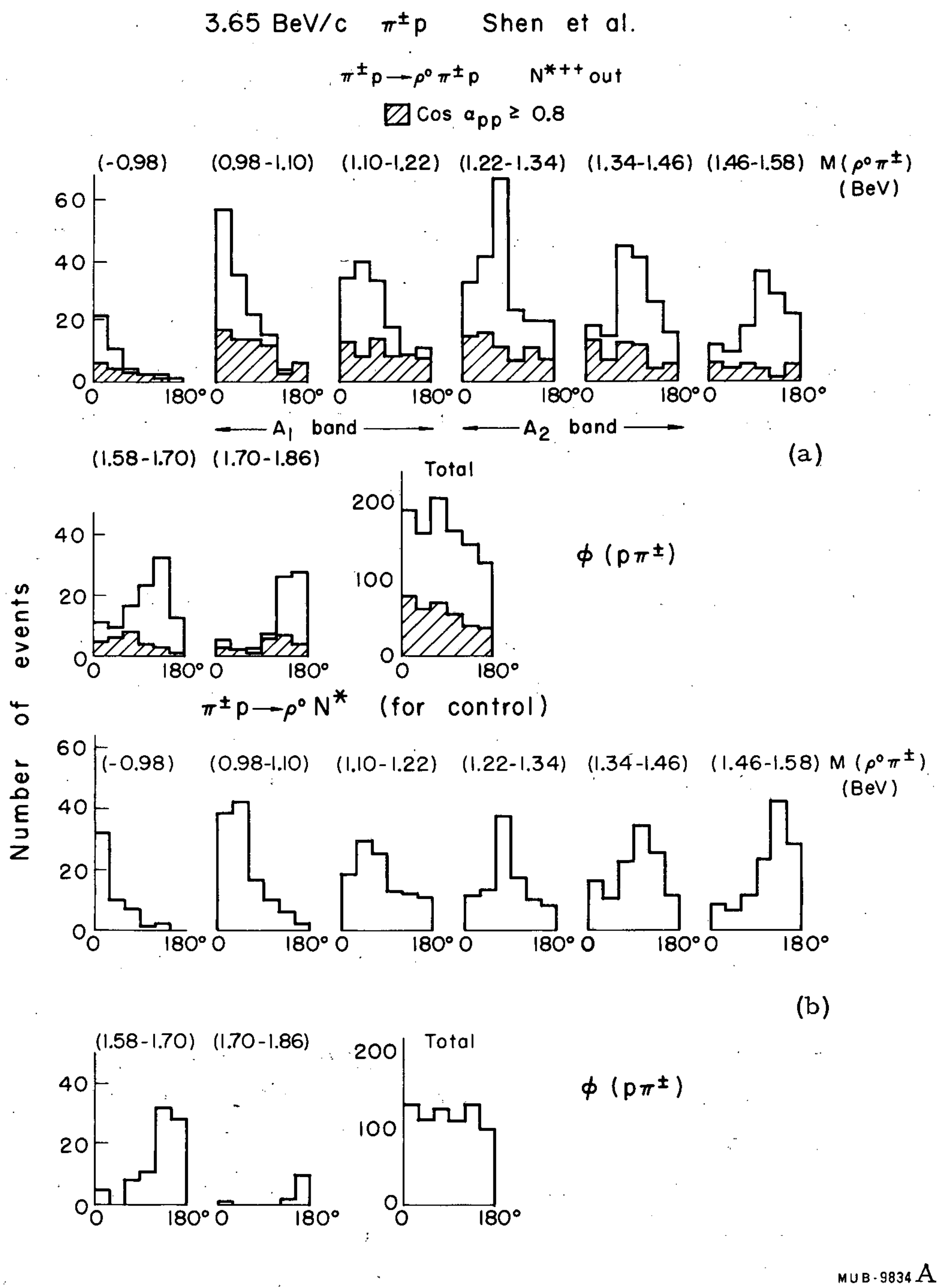

Fig. 21. The Treiman-Yang angular distribution at the outgoing $\pi^{\pm}p$ vertex. (a) Distribution drawn for a selection of $M(\rho^0\pi^{\pm})$ mass values to illustrate the correlations existing between this mass and the Treiman-Yang distribution. (b) The same distribution for $\rho^0 N^*$ events used as a control region.

(ii) When we limit ourselves to events with $\cos\alpha_{pp} \geq 0.8$ (which enhances the A_1 phenomenon), shown shaded in Fig. 21, the $\phi(p\pi^{\pm})$ distribution is nearly consistent with isotropy in the A_1 band.

We thus conclude that the T-Y distribution at the $\pi^{\pm}p$ vertex must be handled with extreme care. When this is done the data do not appear to contradict the "kinematical enhancement" hypothesis.

(d) In Fig. 22 we show the $\Delta^2(\rho^0)$ distribution--the four-momentum transfer to the ρ^0 meson. The distribution for the A_1 band is narrow, the peak extends to $\Delta^2(\rho^0) \approx 30\,m_\pi^2$--however, not so narrow as for $\rho^0 N^{*++}$ events, for example (not shown here). In the latter case the peak extends to $\Delta^2(\rho^0) \approx 10\,m_\pi^2$. A possible interpretation of this difference is given in terms of the kinematical boundary imposed by the Chew-Low plot. This is shown in detail for $K^{**}(1320)$ below.

On the other hand, for the A_2 control band we observe a double "hump" in the $\Delta^2(\rho^0)$ distribution, where the second "hump" $(\Delta^2\rho^0) = 40$ to $80\,m_\pi^2$ is associated with the A_2 meson. Thus the $\Delta^2(\rho^0)$ distribution for the A_1 band may be considered "consistent with the OPE model." For completeness we also show $\Delta^2(p)$, which equals the Δ^2 to the $\rho^0\pi^{\pm}$ system, for the A_1 and A_2 bands (see Fig. 23). If we express these in the form e^{-at}, with $t = \Delta^2(p)$, then we obtain $a(A_1) = 8.3\ (\text{BeV})^{-2}$, and $a(A_2) = 3.0\ (\text{BeV})^{-2}$.

From all the evidence presented here we conclude that the "A_1 enhancement," as observed in our data, is consistent with what is expected from the diffraction scattering of virtual pions.

F. New results from the experiment with 16-BeV/c π^- on Freon

Allard et al.[32] have been able to show from a study of the four-momentum transfer distribution that there is an initial steep slope with t, which they associate with coherent production, followed by a more gentle slope which they associate with noncoherent production (see Fig. 24a). The coherent production gives rise to the A_1 phenomenon exclusively, while the noncoherent production gives the A_1 with the possibility of some A_2 production as well. Figure 24b shows the cross section for the coherent production as a function of the pion mutliplicity. This indicates the great preponderance of 3π production.

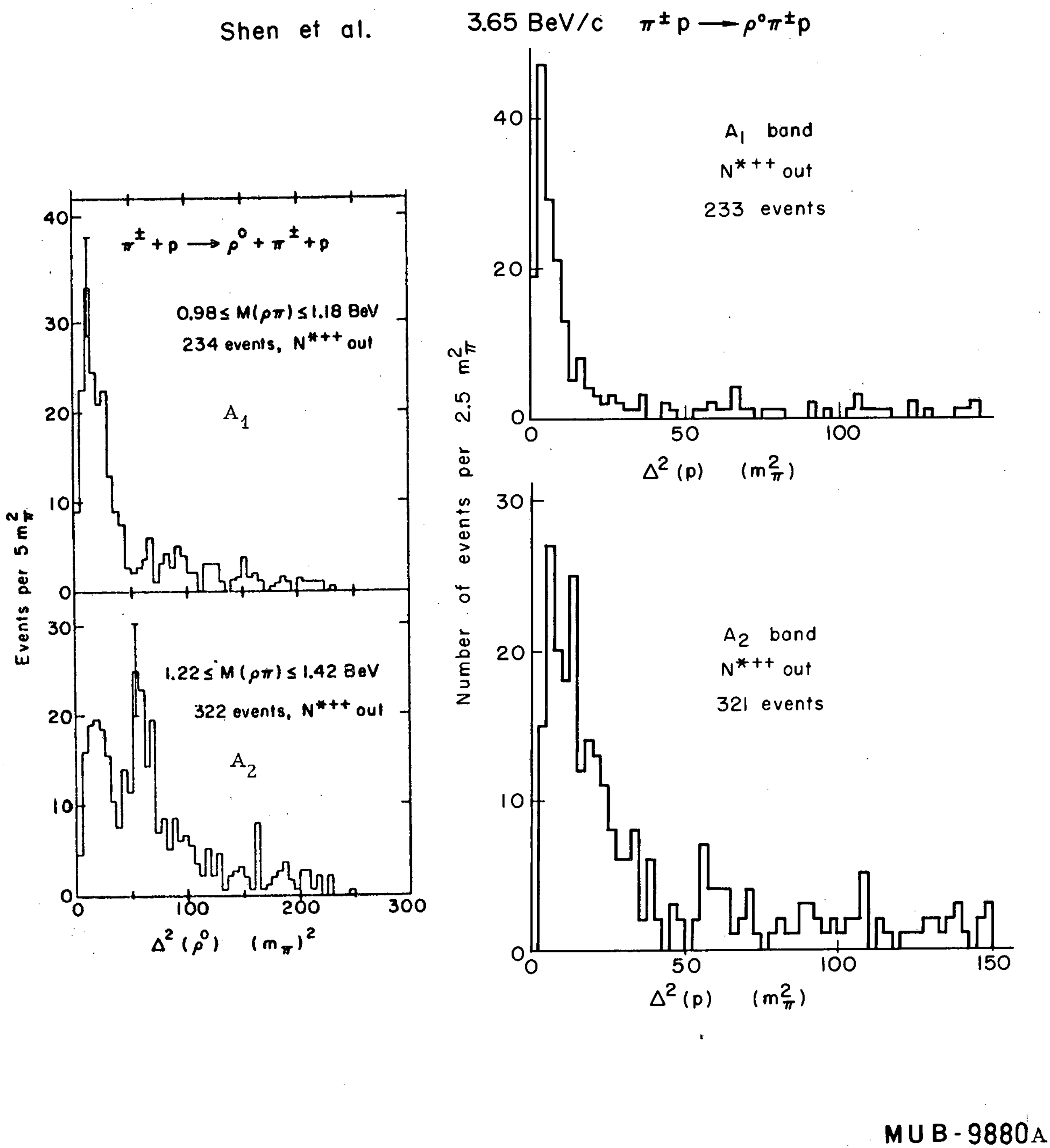

Fig. 22. (left) Momentum transfer to the ρ^0 for the A_1 and A_2 bands respectively.

Fig. 23. (right) Momentum transfer to the $\rho^0\pi^{\pm}$ system for the A_1 and A_2 bands respectively.

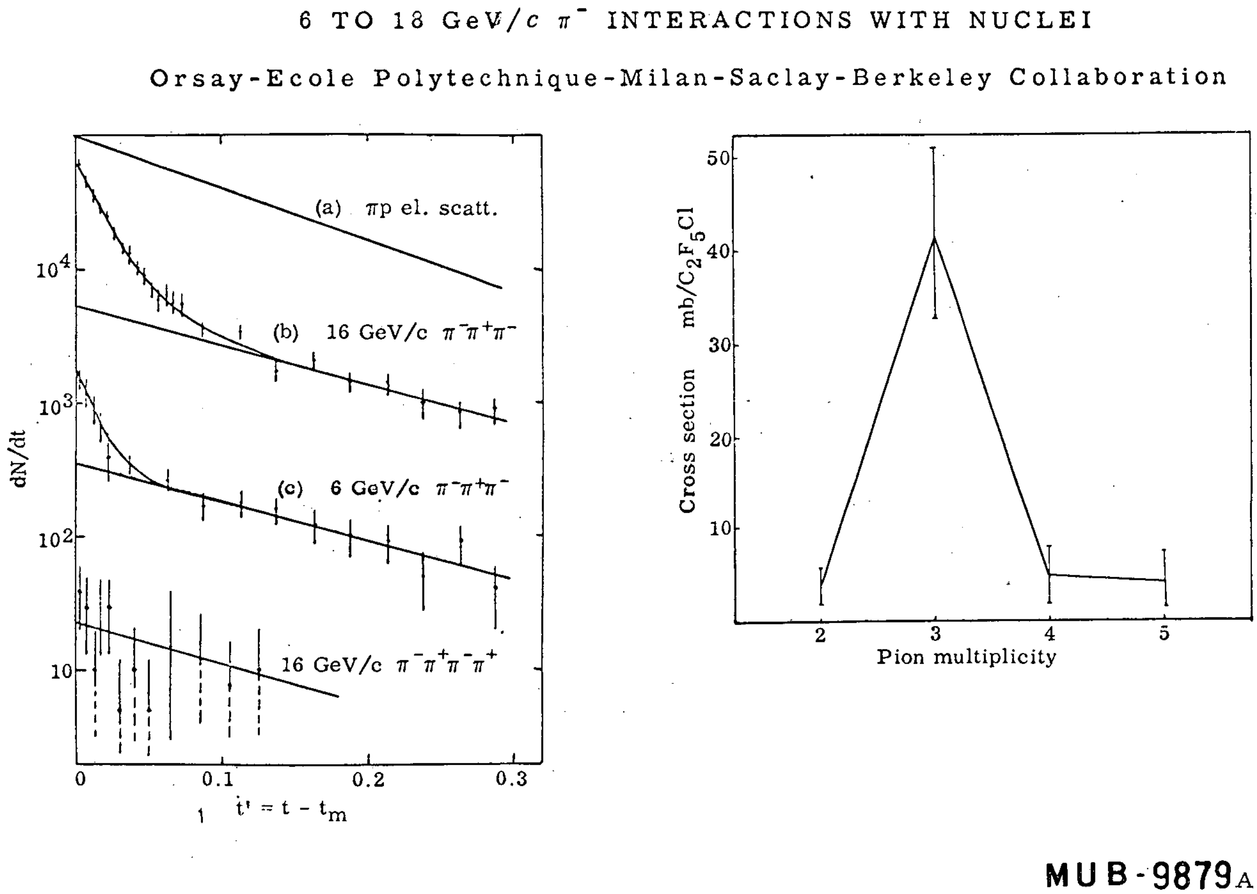

Fig. 24. (left) Logarithmic plot of $d\sigma/dt$ vs t', where $t'=t-t_{min}$. Lines (a), (b), and (c) correspond respectively to $1/t_0$ = 9 $(GeV/c)^{-2}$ (πp scattering), 54 $(GeV/c)^{-2}$ plus a background of 7 $(GeV/c)^{-2}$ (πFl + πn scattering + experimental resolution, least-square fit to data), and 84 $(GeV/c)^{-2}$ plus a background of 7 $(GeV/c)^{-2}$ (πC+πn scattering + experimental resolution, least-square fit to data). (right) Cross section vs pion multiplicity for all channels of charge -1 and $t < (2m_\pi)^2$ for incident π^- of 16 GeV/c.

Huson, as spokesman for the group at the 1966 New York Meeting,[33] also showed the angular distributions they obtain for the ρ^0 decay (see Fig. 25). The results are very similar to our data. They find a very strong alignment of the ρ^0 from the A_1 "decay." which gives a $\cos^2$ distribution together with the well-known forward-backward asymmetry (see Fig. 25a), an isotropic T-Y angle distribution at the ρ^0 vertex (see Fig. 25b), and non-isotropic T-Y distribution at the nucleus vertex (Fig. 25c). The latter distribution was cited by Huson in New York as evidence against the kinematical enhancement hypothesis. However, more recently[34] the fêeling is that this can perhaps be due to contributions from the noncoherent scattering, for which the system may be overconstrained, just as we show for our data above. Furthermore, they give the angular distribution of the "bachelor pion" in the A_1 center of mass with respect to the incident pion (Fig. 25d). This is the same distribution as we show for our data in Fig. 33 below (see discussion in Section VI.2). Finally, they give the Δ^2 distribution to the ρ^0 which they feel is too wide for the OPE model (see Fig. 26), and this together with the narrow width of the A_1 peak, represents at present the only evidence they cite against the kinematical enhancement hypothesis.

G. Compilation by Ferbel

An interesting compilation of all available π^+p and π^-p data was carried out by T. Ferbel[35] (see Table I). He tried to see to what extent the A_1, A_2, and B effects show up if no preselections (such as ρ or ω production, and N^{*++} eliminated) are made.

He compiled data from 2.75 to 8 BeV/c, on two reactions,

$$\pi^{\pm} + p \rightarrow \pi^{\pm} + p + \pi^+ + \pi^-, \qquad \approx 28,700 \text{ events} \qquad (a)$$

and

$$\pi^{\pm} + p \rightarrow \pi^{\pm} + p + \pi^+ + \pi^- + \pi^0, \qquad \approx 26,300 \text{ events.} \qquad (b)$$

His results are that although the A_2 meson persists clearly the A_1 and B "phenomena" are "washed out" to a large extent (see Fig. 27). The results on the B phenomenon are not surprising, as it never showed up noticeably without ω selection. What is particularly relevant here is that the "washing out" of the A_1 peak may indicate small displacements in the peak position in the various momenta compiled. This result favors the kinematic enhancement interpretation for the A_1.

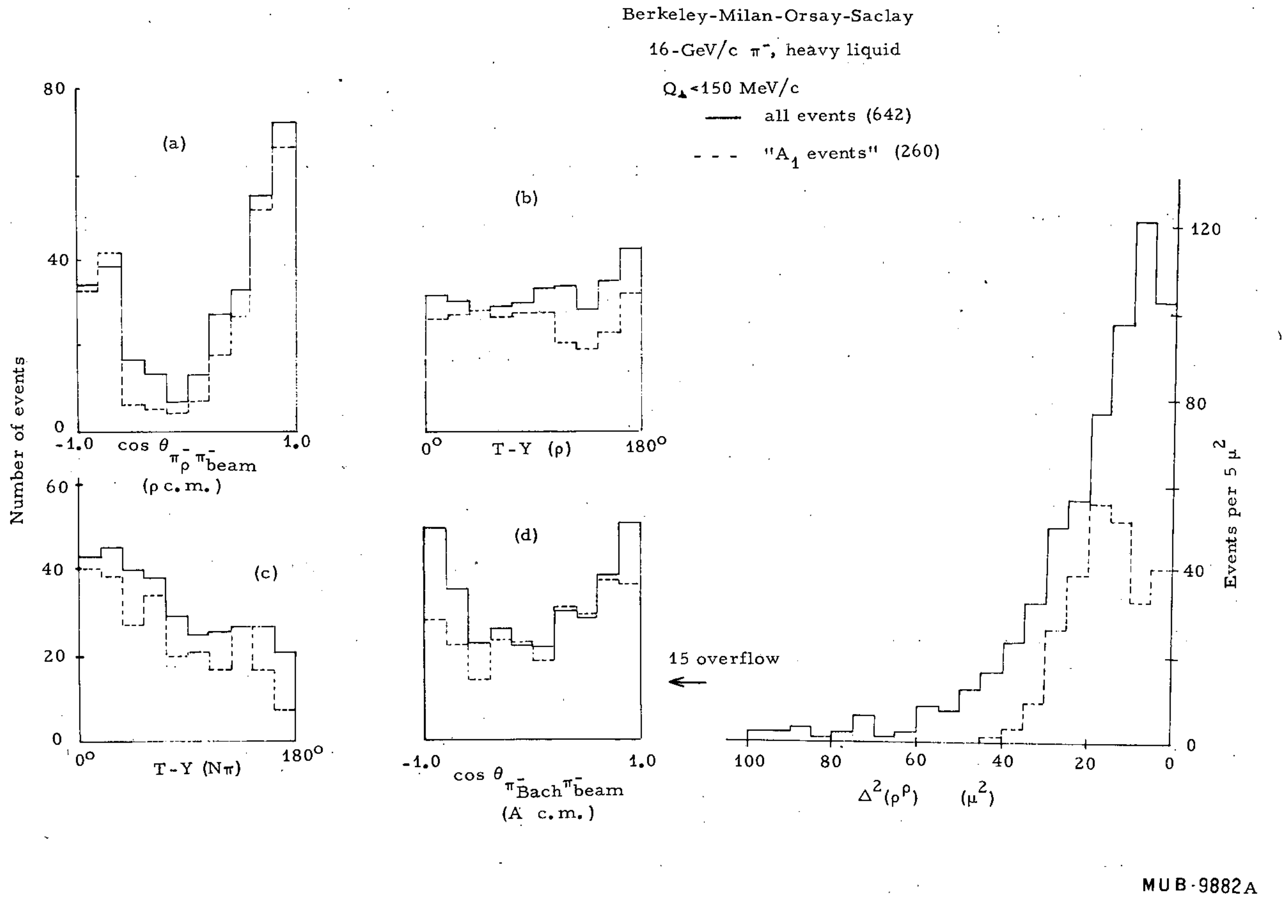

Fig. 25. (left) New data from the π^- on nuclei experiment. (a) The $\pi\pi$ scattering angle in the ρ^0 c.m. (which is called $\cos\alpha_{\pi\pi}$ in the text). (b) The Treiman-Yang angle at the ρ^0 vertex. (c) The Treiman-Yang angle at the π-N vertex. (d) The angular distribution of the ρ^0 (what is actually plotted is the "bachelor pion" direction) with respect to the incident pion in the A center of mass. Dashed curves correspond to the "A_1 events."

Fig. 26. (right) The momentum transfer to the ρ^0. The dashed curves correspond to the A_1 events.

Table I. Sources of the data compiled by Ferbel.

Momentum Range and references (BeV/c)		Number of events			
		π^+ Reactions		π^- Reactions	
		(a)	(b)	(a)	(b)
$\leqslant$ 3.0	a - e	2990	3000	5170	3900
3.0 to 4.0	f - i	5450	5700	6870	7020
$\geqslant$ 4.0	j - n	3840	1800	4420	4900
Total		12280	10500	16460	15820

a. N. Gelfand et al. (Columbia-Rutgers π^+p collaboration).

b. S. S. Yamamoto et al. (Brookhaven National Laboratory π^+p).

c. J. Alitti, J. P. Baton, et al. (S. O. B. B. π^-p collaboration).

d. P. R. Klein, G. Tautfest, et al. (Purdue π^-p).

e. V. Hagopian, W. Selove, et al. (Pennyslvania π^-p).

f. W. Moebs, J. C. Vander Velde, et al. (Michigan π^-p).

g. G. Goldhaber, S. Goldhaber, B. C. Shen, et al. (Berkeley $\pi^\pm p$).

h. M. A. Abolins, P. M. Yager, N. H. Xuong, R. L. Lander, et al. (La Jolla π^+p).

i. S. U. Chung, D. H. Miller, et al. (Berkeley π^-p).

j. A. B. B. B. H. L. M. π^+p Collaboration, Phys. Rev. 138, B897 (1965).

k. N. M. Cason and M. L. Good (Wisconsin π^-p).

l. N. P. Samios et al. (BNL-CCNY π^-p collaboration).

m. K. Lai et al. (BNL-CCNY π^-p collaboration)

n. D. R. O. Morrison et al. (A. B. C. π^+p collaboration).

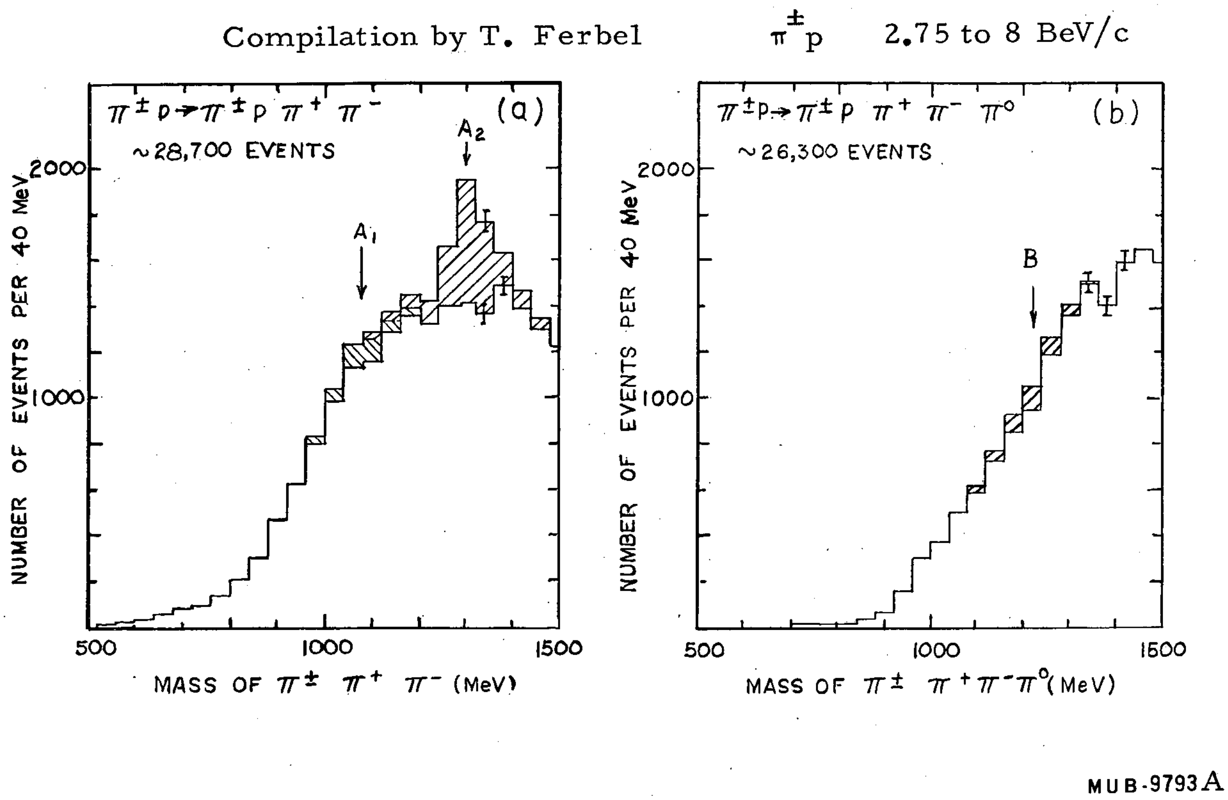

Fig. 27. (a) The $\pi^{\pm}\pi^{+}\pi^{-}$ mass distribution compiled by T. Ferbel without any selection criteria. (b) The $\pi^{\pm}\pi^{+}\pi^{-}\pi^{0}$ mass distribution compiled without any selection criteria.

H. A Test proposed by A. S. Goldhaber

The following comment was made by A. S. Goldhaber.[36] He pointed out that if the A_1 is a meson and consequently a state of definite spin and parity, the ρ meson obtained from A_1 decay should show no forward-backward asymmetry (in the angular distribution of ρ^0 decay) with respect to the incident direction when observed in the A_1 center of mass. It turns out, however, that the transformation to the ρ^0 center of mass does not change the angular distribution drastically, thus even this distribution (in $\cos\alpha_{\pi\pi}$) should not show an asymmetry.

The experimental data, both in our experiment (see Fig. 20) and in the heavy-liquid experiment (see Fig. 25), however, show a very marked asymmetry! The sign and magnitude of the asymmetry are the same as observed for essentially all other sources [no asymmetry in ρ^0 decay is observed in the photoproduction process $\gamma + p \rightarrow \rho^0 + p$ (Ref. 37).] of ρ^0 production by charged mesons.[25] Although one can always invoke interference with a suitable background as the cause for the observed asymmetry, this result favors the kinematical enhancement hypothesis for the A_1.

Although the asymmetry in $K^*(890)$ decay is much less pronounced than for ρ^0 decay, a definite effect has been demonstrated.[38] Here again some asymmetry is obtained for the $K^*(890)$ production from $K^{**}(1320)$ "decay" (see Fig. 29 below).

V. THE EXPERIMENTAL RESULTS AND TESTS ON THE $K^{**}(1320)$ PERTAINING TO KINEMATIC ENHANCEMENT

All the arguments and graphs we gave for the A_1 can be repeated here for $K^{**}(1320)$. We will just present the corresponding figures from our 4.6-BeV/c K^+p experiment with very few comments.* Figure 28a shows the Dalitz plot for all K^* events from Reactions (1) and (2). In Fig. 28b we show the scatter plot for these same events of $M^2(p\pi)$ versus $\cos\alpha_{pp}$. From this it can be seen clearly that the $K^{**}(1320)$ band corresponds to the

*Similar results on some of these angular distributions have been obtained by the group at Oxford from a study of the K^-p interaction. (private communication from D. H. Locke to S. Goldhaber). Graphs on their work are, however, not available to us at present.

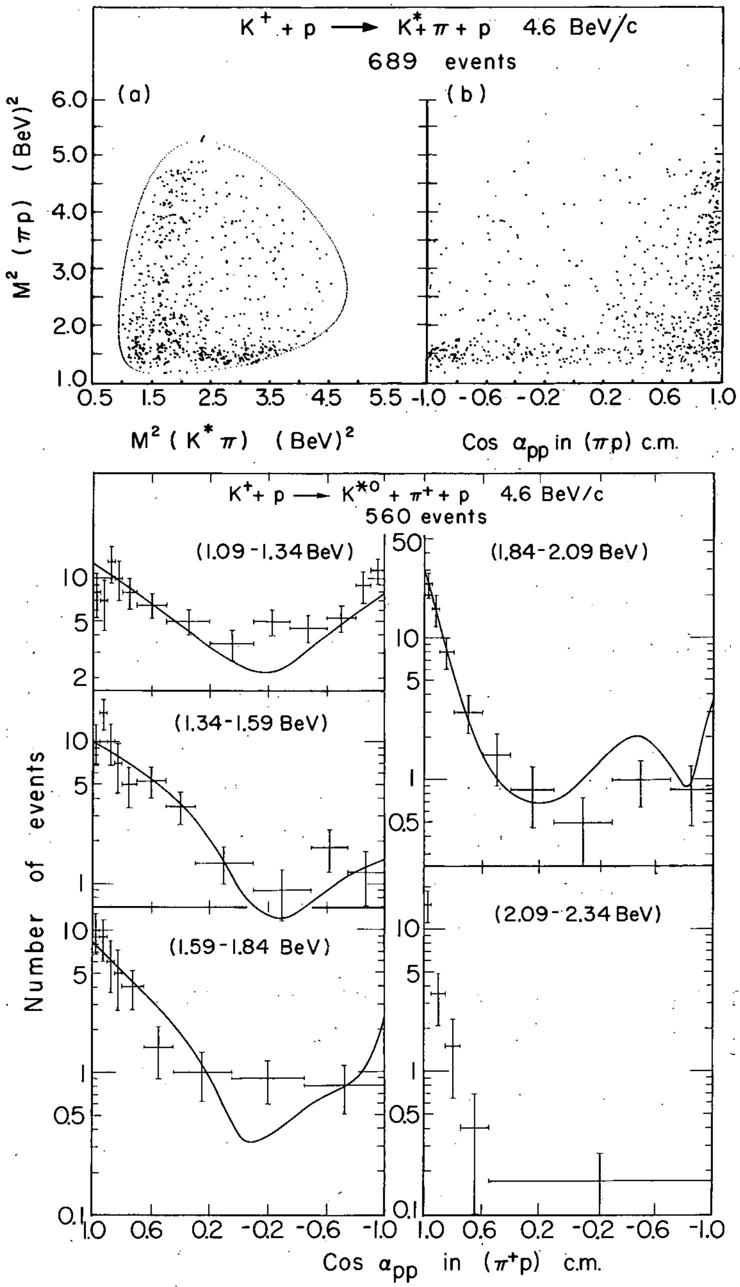

MUB-9786

Fig. 28. (a) The Dalitz plot for all $K^*\pi p$ events from the 4.6-BeV/c data. This corresponds to the sum of the Dalitz plots shown in Fig. 8. (b) The same events as in (a) shown in a scatter plot of the $M^2(\pi p)$ vs $\cos\alpha_{pp}$. The comparison between (a) and (b) indicates that the $K^*\pi$ enhancement corresponds to the observed enhancement at small α_{pp} scattering angles. (lower) The $\cos\alpha_{pp}$ distributions for a selection of π^+p mass bands similar to Fig. 18, which is drawn for the A_1 phenomenon. The curves shown come from the available counter experiments averaged over the energy intervals indicated. In the plots shown here no Δ^2 cutoff was taken.

small-angle band ($\cos\alpha_{pp} \approx 1$). Figure 28 also shows the $d^2\sigma/d\Omega dM$ distribution (in arbitrary units). These are compared with the experimental curves for $\left\langle \frac{d\sigma_{el}}{d\Omega} \right\rangle$. This figure is the analog to Fig. 18, corresponding to the point (e) in Section IIIA. Figure 29 shows the $\cos\alpha_{KK}$ distribution in the K^* center of mass and also the T - Y distribution at the K^* vertex for events in the $K^{**}(1320)$ band. Also shown as a control region are the same distributions for $K^{*0}(890)\, N^{*++}$ events. As expected on the Deck model, the two sets of distributions are very similar. Figure 30 gives the T - Y distribution at the π^+p vertex. Here again this distribution is anisotropic, where the anisotropy is associated with the $K^*\pi$ mass cuts. The same distribution for the $K^{*0} N^{*++}$ events, here shown as a control region, also gives this correlation. In Fig. 31c we show the $\Delta^2(K^*)$ distribution for events in the $K^{**}(1320)$ band. At first sight this distribution looks too broad for the OPE model, say, when compared with the control region for $K^* N^{*++}$ events in Fig. 31d. A possible explanation for this broad distribution is, however, quite straightforward. It becomes clear if we look at the Chew-Low boundary calculated for $K^*\pi p$ production [using $M(K^*)_{min}$ = 840 MeV, the lower limit of the K^* mass band] in Fig. 31a. Thus the events with high π^+p masses, which contribute appreciably to the $K^{**}(1320)$ band, are forced by the kinematic boundary to lie at fairly high $\Delta^2(K^*)$ values, while the events in the N^{*++} band (Fig. 31b) are not so constrained.

Finally, for completeness we also give $\Delta^2(p)$, which is the same as the Δ^2 to the $K^*\pi$ system. If we represent this in the form e^{-at}, with $t = \Delta^2(p)$, then we find $a(K^{**}) = 6.7\ (\text{BeV})^{-2}$.

Here we must stress that the boundary shown in Fig. 31a corresponds to the "minimum values" of the K^* mass. If we draw the boundary for the "maximum value" (940 MeV, not shown here) it comes much closer to the points at high $M(p\pi)$ values. All the same, even a distribution in $\Delta^2(K^*) - \Delta^2(K^*)_{min}$ remains slightly broader than for K^*N^* events, where $\Delta^2(K^*)_{min}$ is the Chew-Low boundary value for a given event [i.e., a function of $M(p\pi^{\pm})$ and $M(K\pi^-)$ for the event].

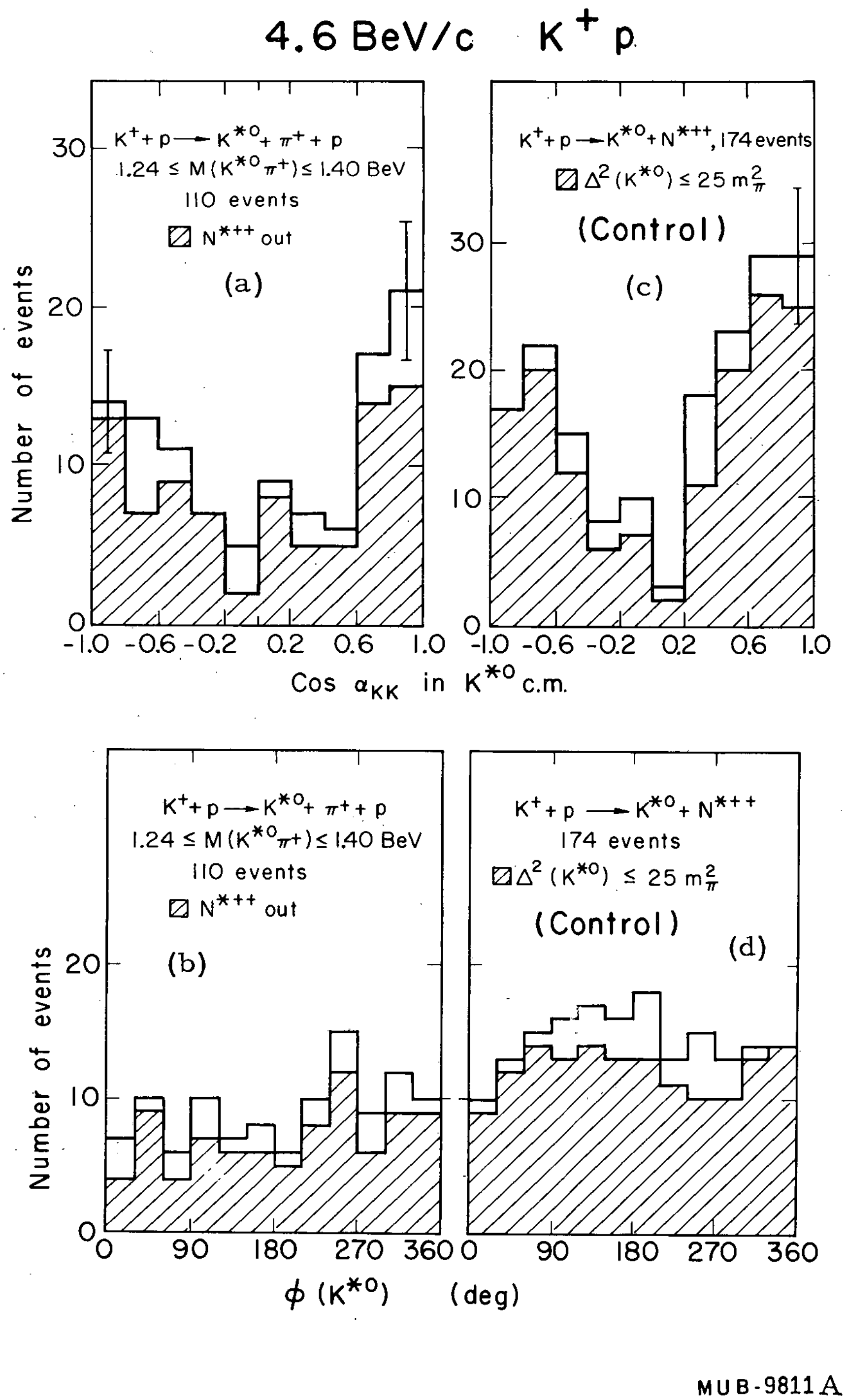

Fig. 29. (a) The KK scattering angle in the K^{*0} center of mass, and (b) the Treiman-Yang angle at the K^* vertex; (c) and (d), corresponding distributions for the K^*N^* events.

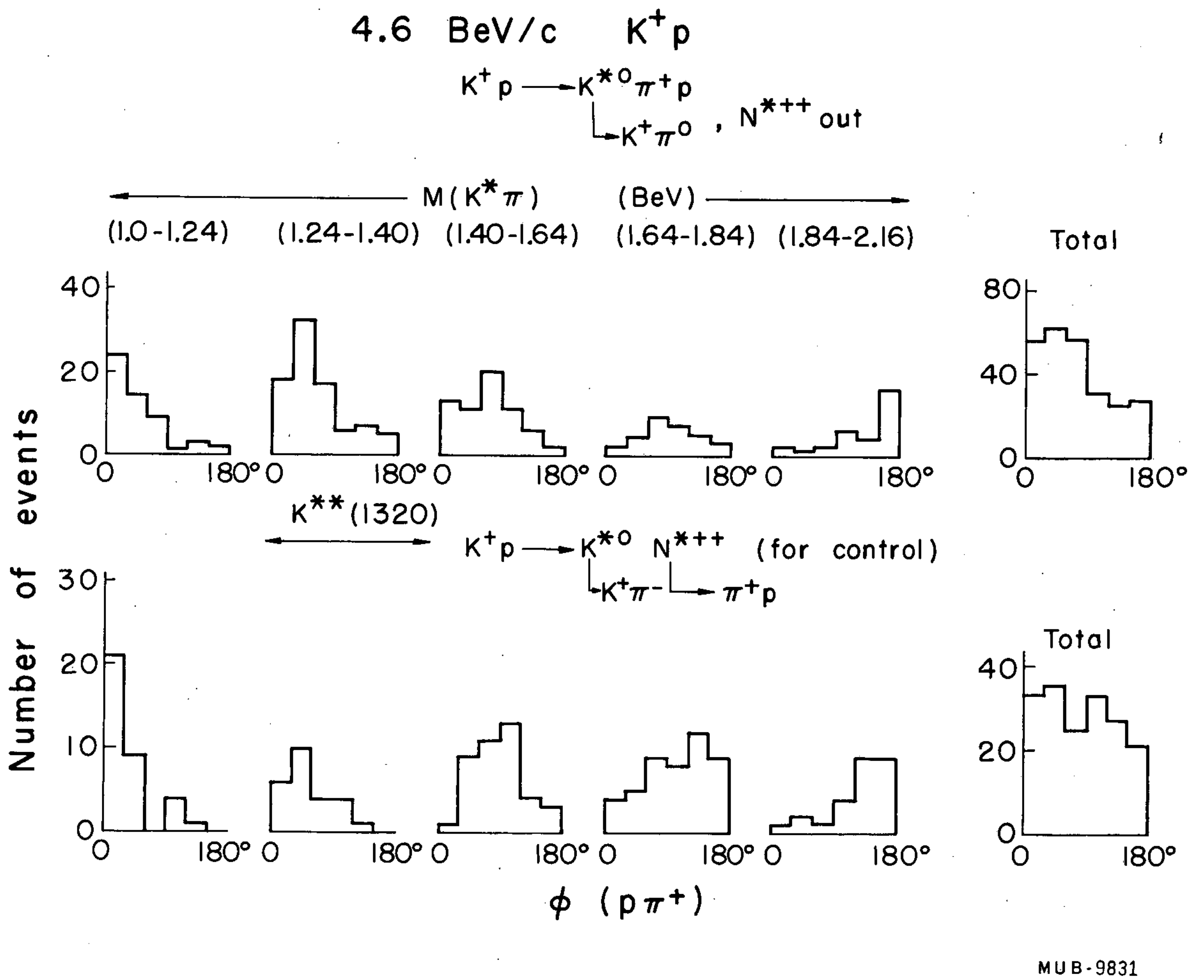

Fig. 30. (upper) The Treiman-Yang angle distribution at the proton vertex. The distributions were drawn for a selection of $M(\rho^0 \pi^{\pm})$ mass values, to illustrate the correlation between this mass and the Treiman-Yang distribution. (lower) The same distribution for $K^{*0} N^{*}$ events used as a control region.

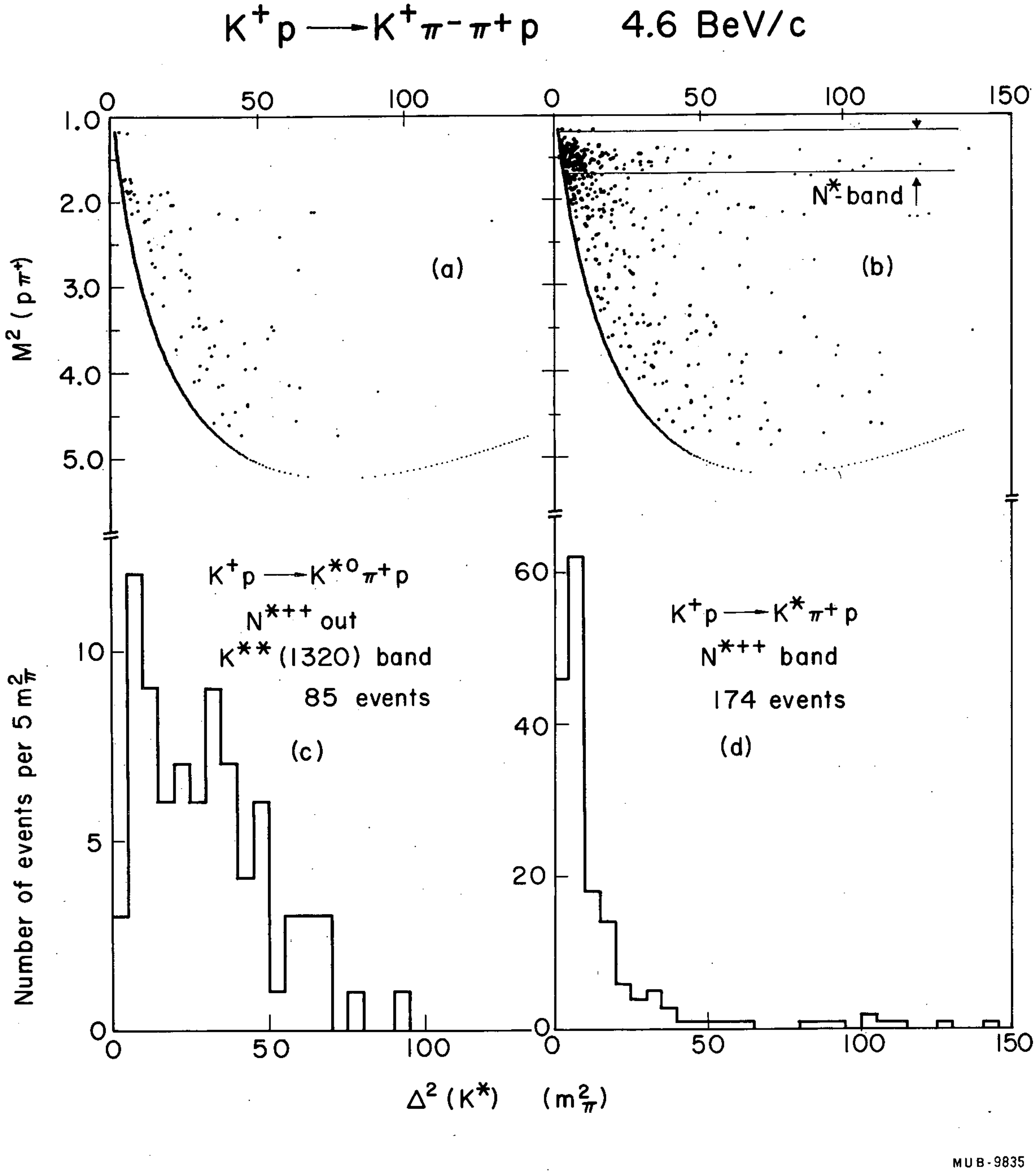

Fig. 31. Distribution of the four-momentum transfer to the K^*. The Chew-Low plot shown in (a) indicates how the boundary forces the events to higher $\Delta^2(K^*)$ values.

Data presented by Dornan et al.[39] at the 1966 Washington Meeting is of particular relevance to the subject under discussion here. Dornan et al. studied the K^-p reaction at 4.6 BeV/c.

In particular they observed $K^*(890) + \pi$ production in the reactions

$$K^-p \to \overline{K}^0 \pi^- \pi^0 p \tag{8}$$

$$\to \overline{K}^0 \pi^- \pi^+ n. \tag{9}$$

In these reactions $K^*(890)$ production occurs according to

$$K^-p \to \overline{K}^{*-} \pi^0 p \tag{8a}$$

$$\to \overline{K}^{*0} \pi^- p \tag{8b}$$

$$\to \overline{K}^{*-} \pi^+ n. \tag{9a}$$

These reactions differ markedly if interpreted in terms of the Deck Mechanism. In Reactions (8a) and (8b) we can consider the lone pion to undergo diffraction scattering at the proton vertex; however, in Reaction (9a), on this model, the exchange pion must undergo charge-exchange at the proton vertex. This tends to reduce the cross section very considerably. The experimental data (see Fig. 32) indeed shows a very considerable peak in the $K^*(890)\,\pi$ mass distribution near 1320 MeV for Reactions (8a) and (8b) combined, but not for Reaction (9a)! On the other hand, evidence for $\overline{K}^*(1400) \to \overline{K}^*(890) + \pi$ is observed in both reactions. These data thus strongly favor the kinematical enhancement interpretation for the $K^{**}(1320)$. Although one might be tempted to close the subject right here, there is one "out" left to the "meson hypothesis." All reactions other than (9a) leading to $K^{**}(1320)$ production (considered now as meson) can proceed via isoscalar exchange, whereas Reaction (9a) must correspond to isovector exchange. If for some reason the latter is strongly supressed relative to the former, one could also explain the data shown in Fig. 32 on the "meson hypothesis."

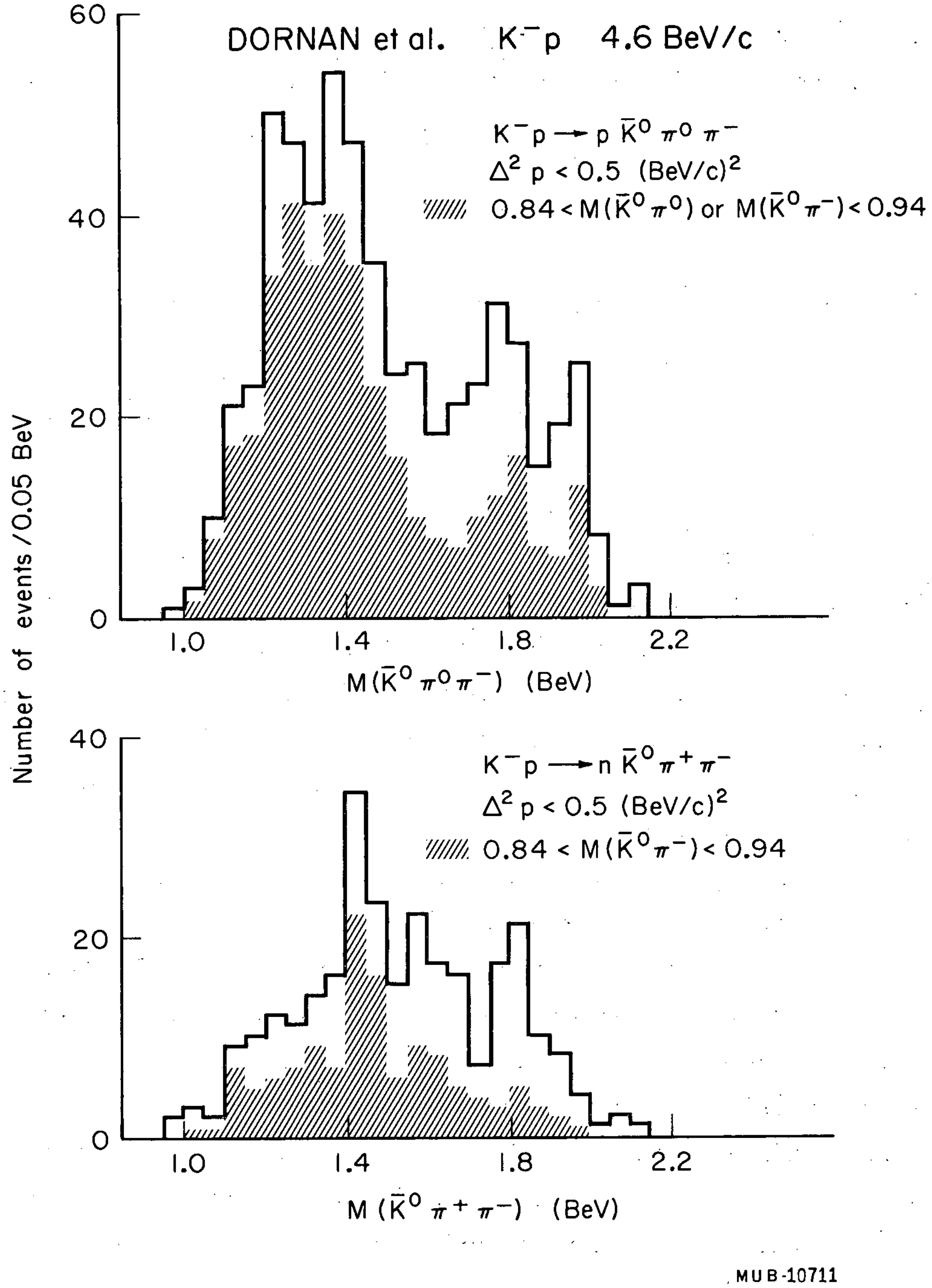

Fig. 32. Results of work by Dornan et al. (Reference 39).

VI. THE ARGUMENTS IN FAVOR OF AN A_1 MESON AND $K^{**}(1320)$ MESON

1. Spin assignment from the A_1 Dalitz plot

As pointed out by Zemach[40] and Frazer et al.,[41] and from the numerical evaluations by Diebold,[42] if we are dealing with a definite $\pi\rho$ state the J^P value can (in principle) be obtained from a Dalitz plot. Figure 33 shows the data of the 8-BeV/c π^+p experiment[7] and the 16-BeV/c π^- on Freon experiment[1] relating to this question. These results favor the assignments $J^P = 1^+$, with 2^- as a less likely possibility.

2. Leith's argument favoring a $J^P = 1^+$ A_1 meson

During a seminar by one of us at CERN (October 1965) on our A_1 data, D. Leith[43] pointed out that the observed alignment of the ρ^0 from the A_1 band with the incident direction could also come from a 1^+ meson. He makes the point that one could have A_1 production (considered here as a $J^P = 1^+$ meson) by a diffraction effect involving the exchange of a 0^+ "object" or the vacuum trajectory on the Regge formalism. This would lead to an alignment of the A_1, since it would be produced from a collision between a 0^- meson and a 0^+ "object" in a relative p state. The argument is identical to the alignment obtained for a ρ^0 meson in virtual pion exchange. Next the A_1 decays through an s wave into a ρ^0 and π. Thus the ρ^0 would carry the same alignment as the A_1 and hence would show the characteristic $\cos\alpha^2_{\pi\pi}$ distribution we observe. There is a fine point involved here, namely the A_1 is completely aligned in the A_1 center of mass, while the ρ^0 alignment is studied in the ρ^0 center of mass. The transformation between the two centers of mass is such, however, that the alignment is not appreciably altered. This also applies to the T-Y angle at the ρ^0 vertex, which, strictly speaking, would be expected to be isotropic only for the A_1 polarization vector in the A_1 center of mass.

Thus this model would satisfy conditions (a) and (b) of Section IIIA. Furthermore Leith argues that our data indeed correspond primarily to diffraction scattering of the virtual pion, as we have suggested, and that the A_1 meson is superimposed on a considerable background. Thus all other observed features remain unaltered.

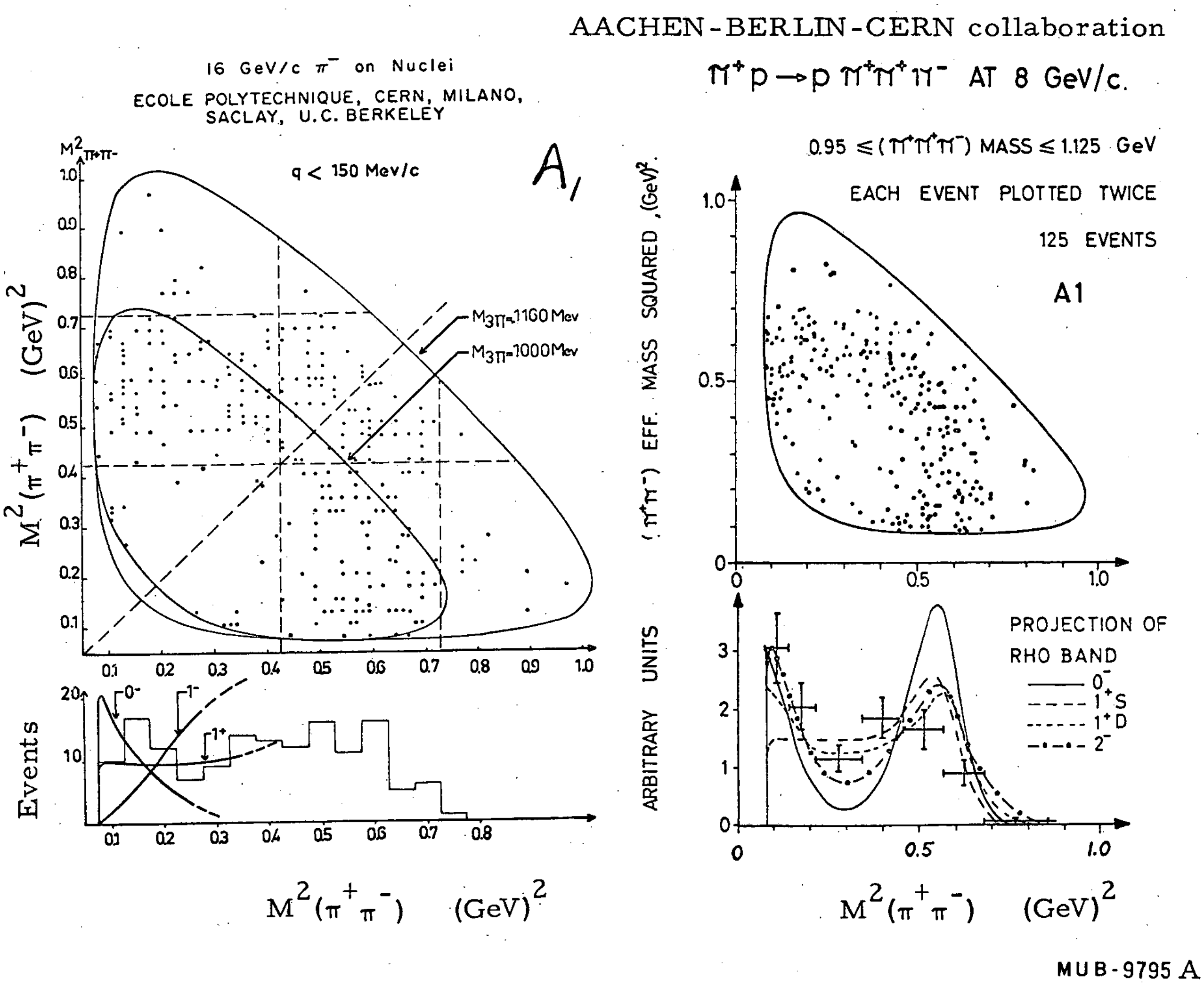

Fig. 33. The Dalitz plots for the A_1. These show the evidence for spin assignments if the A_1 is considered a meson.

Finally, on Leith's model, since A_1 decay into $\pi\rho$ (and similarly K^{**} into $K^*\pi$ if this is also considered as a 1^+ meson) proceeds via an s wave, the distribution of the ρ^0 in the A_1 center of mass should be isotropic relative to, say, the incident π direction. In Fig. 34 we show this distribution for the A_1 and K^{**} bands (as well as the A_2 band for control). Figure 25d shows the same distribution for the heavy-liquid experiment. As may be noted, the distributions are not far from isotropic, although they appear to have a small $\cos^2$ component present. Thus here again it becomes a quantitative question as to how much background and how much of the A_1[or K^{**}(1320)] meson is present. No definitive conclusion can be drawn on the basis of presently available data.

3. <u>The sharp A_1 peak in the 8-BeV/c data</u>

As shown in Fig. 4, the A_1 peak observed in this experiment is very sharp, and as such is suggestive of a bona fide resonance. There are, however, two questions to be answered: (a) Why is this effect not so clear in the 6-BeV/c π^-p data? (b) To what extent can we believe the OPE calcualtions by Wolf[44] (unpublished) for an accurate background subtraction? Does one really know how to calculate the OPE model (including Bose symmetrization) for higher spin resonances, such as the $N^*_{3/2}$(1920) in this case?

4. <u>The Sharp K^*(1320) peak in the 4.6-BeV/c K^+p data</u>

In our data[11] (see Fig. 8) we also observe a rather sharp $K^*\pi$ peak. But the same criticisms applied to the A_1 peak apply here as well: (a) Why do the data of Jongejans et al.[12] (at other incident K^+ momenta) not show such a sharp peak? (b) We do not know the accurate detailed shape for this peak to be expected from an OPE model. One small point here, which favors the "meson" hypothesis, is the location of the peak. From the OPE calculations (e.g., Maor and O'Halloran) one obtains an expected mass of ≈ 1200 MeV for such a peak. This is also the value obtained from a crude order-of-magnitude estimate in which we consider that on an OPE model the "Q value" for $A_1 \to \pi + \rho$ should be the same as that for $K^{**} \to \pi + K^*$. Thus the experimental value of 1320 MeV is about 100 MeV higher than the OPE value. As mentioned in (b), however, it is conceivable that there is that much leeway between the present-day OPE calculation and a "correct" calculation.

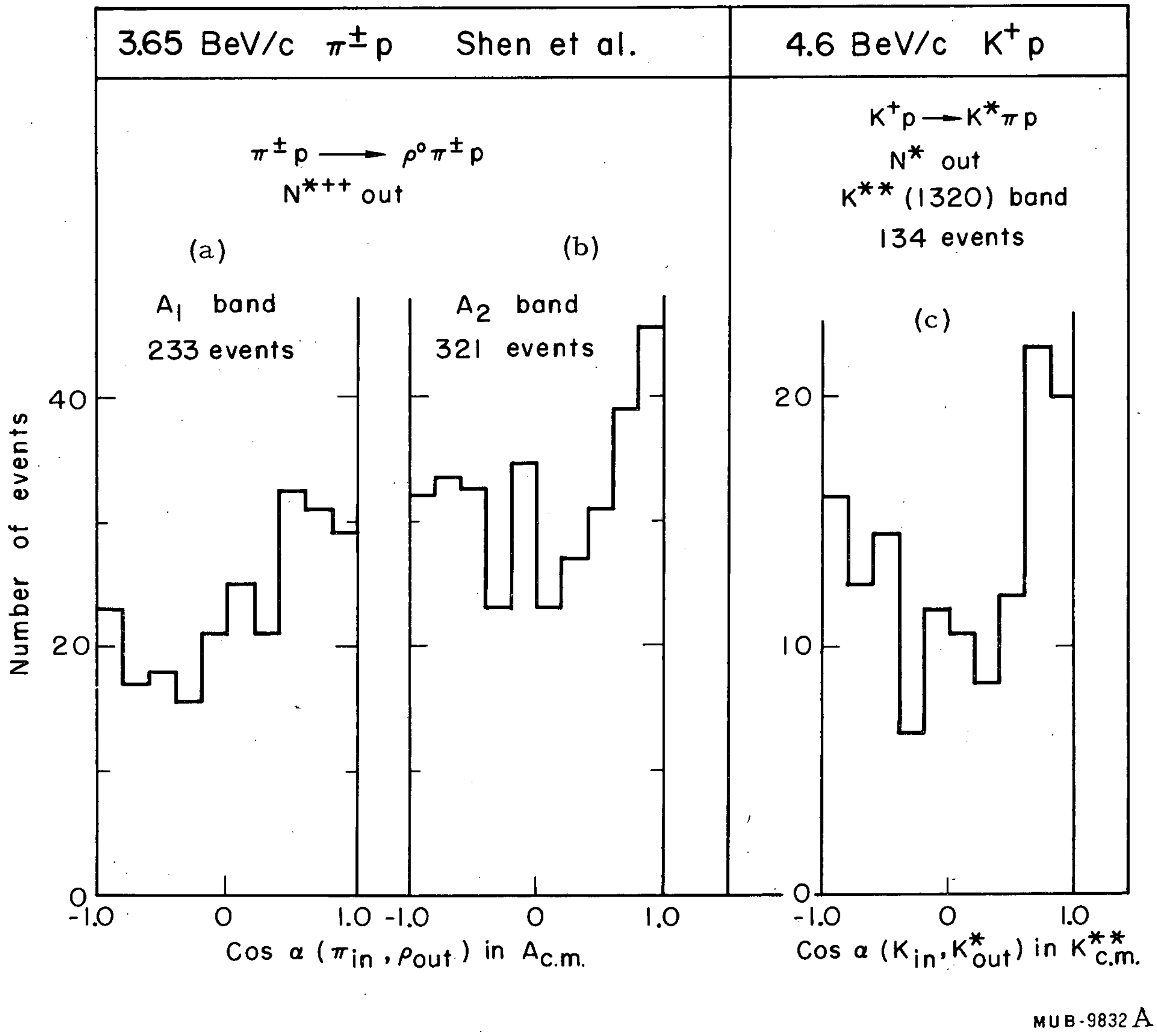

Fig. 34. (a) and (b) Angular distribution of the ρ^0 with respect to the incident direction in the A center of mass for the A_1 and A_2 bands. (c) Corresponding distribution for the $K^*(890)$ in the $K^{**}(1320)$ center of mass.

VII. "COHERENT" $\rho^0\pi$ AND $K^*\pi$ PRODUCTION ON DEUTERIUM

There is a recent series of experiments on the $\pi^\pm$ D interaction and K^+D interaction which have observed $\rho^0\pi^\pm$ production and $K^{*0}\pi^+$ production, respectively, without deuteron breakup:

$$\pi^\pm d \to \rho^0 \pi^\pm d$$
$$K^+ d \to K^{*0} \pi^+ d$$

The experiments are:

π^-D at 3.2 BeV/c	Miller et al.[45]	(Fig. 35),
π^-D at 3.7 BeV/c	Abolins et al.[46]	(Fig. 36),
π^+D at 6 BeV/c	Vegni et al.[47]	(Fig. 37),

and our own experiment,

K^+D at 2.3 BeV/c	Butterworth et al.[48]	(Fig. 38).

These experiments show a number of features of relevance here.

a. In each of the experiments, ρ^0 (or K^*) production is the dominant process [from 80 to 100% of all $\pi^\pm\pi^+\pi^-$ d) events]. See the $\pi^+\pi^-$ (or $K^+\pi^-$) distributions in Figs. 35 through 38.

b. The ρ^0 and K^* are observed to be aligned in the respective experiments (see Figs. 35 and 38).

c. The respective experiments show $\rho^0\pi^\pm$ mass peaks and a $K^*\pi$ mass peak which are very broad. The $\rho^0\pi$ data do not show any A_1 or A_2 structure, neither does the $K^*\pi$ peak show a K^{**}(1320) structure (see Figs. 35 through 38). The location of the A_1 and A_2 peaks has been indicated on Figs. 35 through 37.

The mechanism by which these reactions occur is not fully understood at present. There are three possible mechanisms we can consider:

(a) In each of the reactions observed, $\rho^0\pi^\pm$ (or $K^*\pi$) production with deuteron breakup is an important channel. The observed data may thus correspond to the very low-momentum-transfer end of these reactions (possibly even with pn recombination to form a deuteron). In this case the deuteron (without breakup) is acting as a "momentum transfer filter" which ensures small momentum transfer to the deuteron and consequently to the

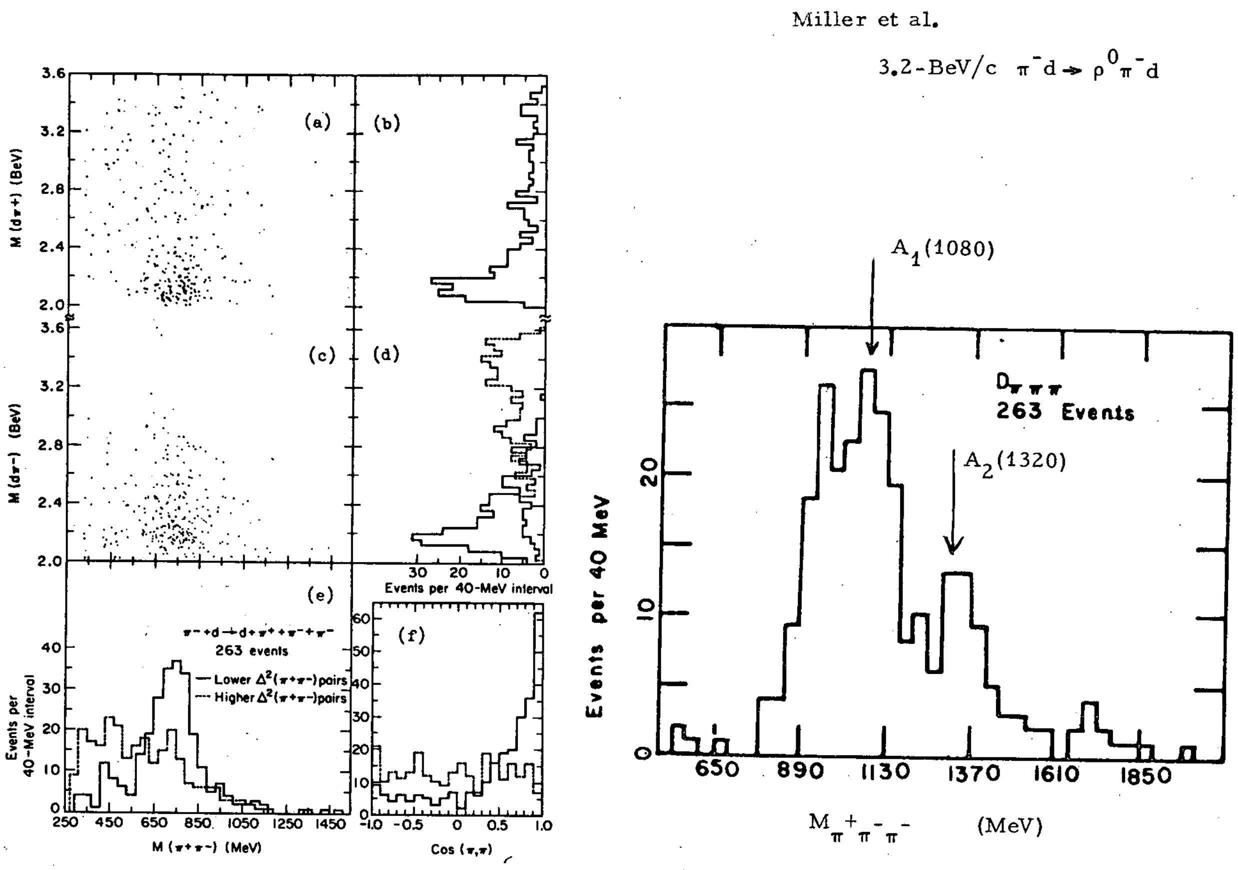

MUB-10191

Fig. 35. (left) (a)-(e). Scatter plots and effective-mass projections for $\pi^-+d\rightarrow d+\pi^++\pi^-+\pi^-$. The scatter plots include only the combination $\pi^+\pi^-_1$. (d) and (e) include also the combination $\pi^+\pi^-_2$ (see text). (f) The distribution in $\cos\theta$ of the angle between the incident pion and the outgoing π^- in the $(\pi^+\pi^-)$ center of mass for both $\Delta^2(\pi\pi)$ combinations. (right) The effective-mass distribution for the three pions in the final state, $d+\pi^++\pi^-+\pi^-$.

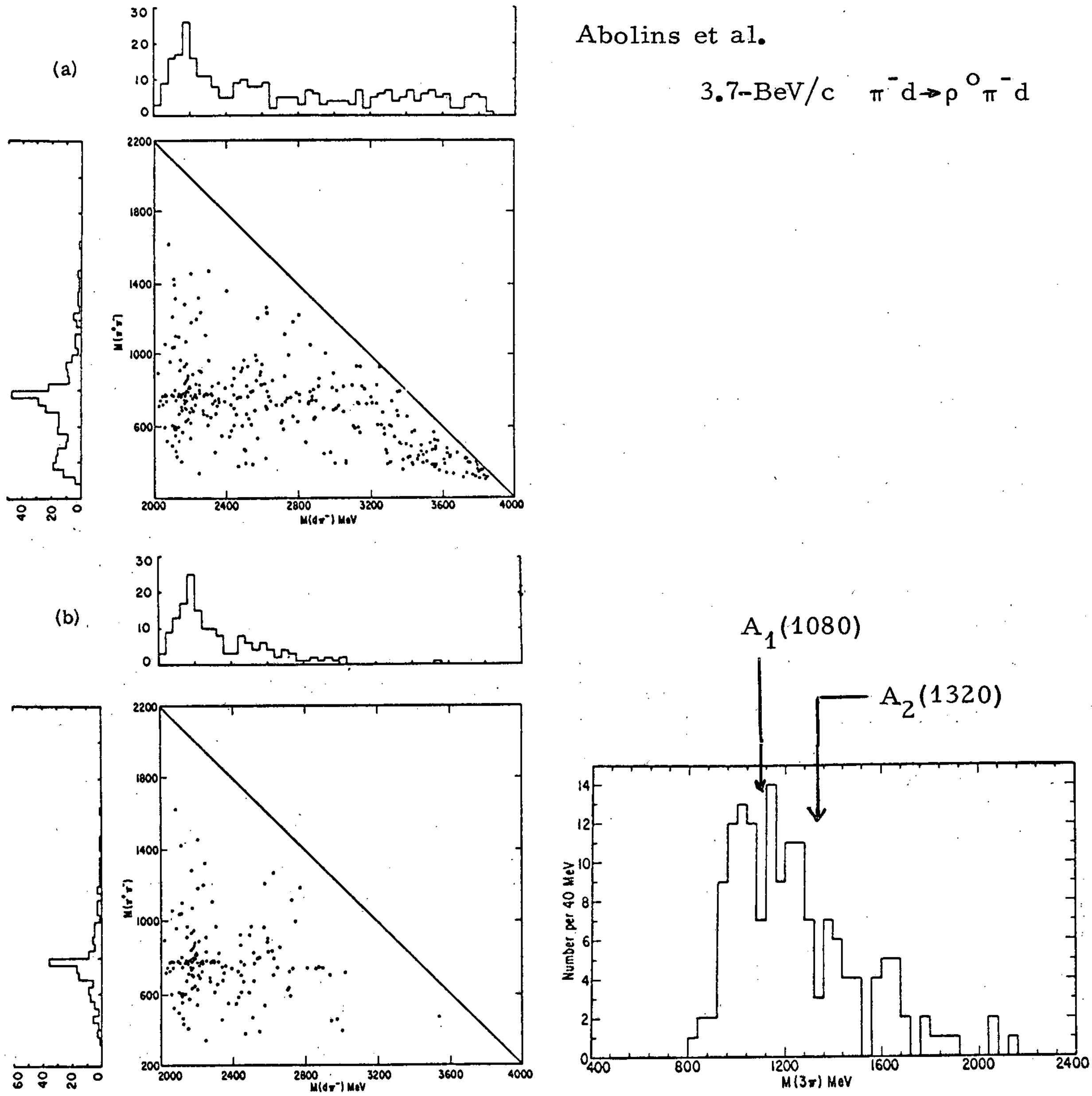

MUB-10192

Fig. 36. (left) (a) Histogram of the d-π_1^- mass versus π_2^- - π^+mass. Each event is plotted twice. (b) Histogram of the d-π_1^- mass versus π_2^- - π^+ mass. Each event is plotted once. π_2^- is the π^- which gives the lower momentum transfer to the π^+ - π_2^- combination. The reaction studied was $\pi^- d \rightarrow \pi^- \pi^+ \pi^- d$, but led primarily to $\rho^0 \pi$-d formation. (right) Distribution of effective mass of the three pions; all events.

Fig. 37. (left) (a) Distribution of the quadrimomentum transfer t to the deuterium; solid line: 251 events that fit $\pi^+ d \rightarrow d\pi^+\pi^+\pi^-$. (b) Distribution of the square of the transverse momentum $q_\perp$ given to the deuterium in the reaction $\pi^+ d \rightarrow d\pi^+\pi^+\pi^-$; solid line: the 251 four-prong events, and the 56 three-prong events (shaded events), fitting $\pi^+ d \rightarrow d\pi^+\pi^+\pi^-$; dashed line: the four-prong events with $M^*\pi^+ d \leq 2.35$ $(\mathrm{GeV}/c)^2$. The exponential fits to the graphs are made over the interval 0.02 - 0.1 $(\mathrm{GeV}/c)^2$ for (a) and (b) and over the interval 0.0 - 0.1 $(\mathrm{GeV}/c)^2$ for (c). For comparison, on (c), the corresponding lines have been drawn for radii of proton (R = 1.1 F) and of carbon (R = 3.24 F). (c) Distribution of the quadrimomentum transfer t to the deuterium of 570 elastic $\pi^+ d$ events, corrected for scanning bias (preliminary results).
(right) (a) Effective mass of the three pions in the reaction $\pi^+ d \rightarrow d\pi^+\pi^+\pi^-$. Shaded events are the ones with $M^*(\pi^+ d) < 2.35$ $(\mathrm{GeV}/c)^2$. (b) $\pi^+\pi^-$ effective-mass distribution, each event plotted twice. Dotted events are the combinations which give a $\pi^+\pi^-$ mass further from the ρ mass. (c) $\pi^+_A\pi^-$ invariant-mass distribution, taking the π^+ which, associated with the deuterium, leads to the lower quadrimomentum transfer to the system $\pi^+ d$. Dashed events are the ones with $M^*(\pi^+_A d) < 2.35$ $(\mathrm{GeV}/c)^2$.

Vegni et al.   6-BeV/c $\pi^+ d \rightarrow \rho^0 \pi^+ d$

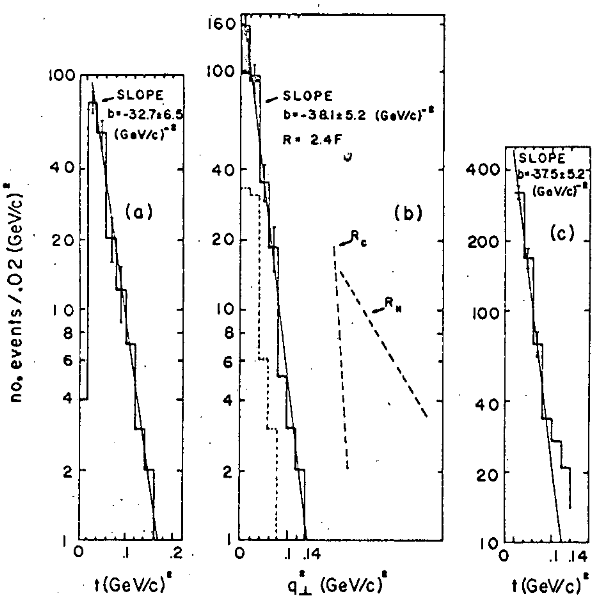

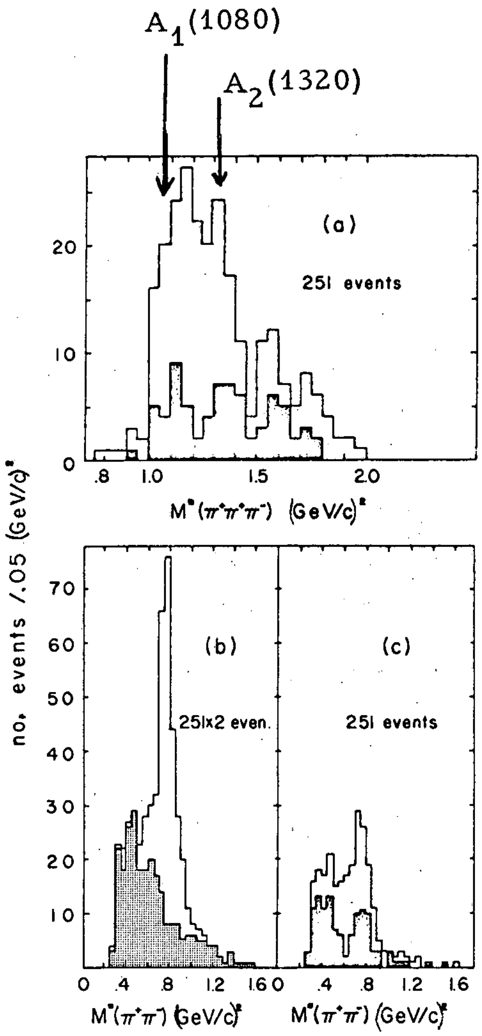

MUB-10193

Fig. 38. (a) $M_{d\pi^+}$ vs $M_{K^+\pi^-}$ for the reaction $K^+ + d \to K^+ + \pi^- + \pi^+ + d$, with projections. For the $M_{d\pi^+}$ projection the shaded histogram shows the distribution for events with $M_{K^0\pi^+}$ in the K^* region (0.84 to 0.96 Bev). The solid and dashed curves show phase space for $K+d \to K+\pi+\pi+d$ and $K+d \to K^*+\pi+d$, respectively, normalized to the appropriate number of events. (b) The reaction $K^+ + d \to K^+ + \pi^- + \pi^+ + d$. Distribution of $\cos \alpha_{K^*} = (|K_{in} \cdot K_{out}|)/(|K_{in}||K_{out}|)$, the cosine of the $K\pi$ scattering angle in the $K\pi$ center of mass, for events with $0.84 \leq M_{K\pi} \leq 0.96$ BeV. (c) The reaction $K^+ + d \to K^+ + \pi^- + \pi^+ + d$. Chew-Low plot of $\Delta_{K\pi\pi}^2$ vs $M_{K\pi\pi}^2$. The solid points are for events with $0.84 < M_{K^+\pi^-} < 0.96$ BeV, i.e., in the K^* region. Those marked $\times$ are for events outside this region. Shaded histograms refer to the former events. The smooth curve on the $M_{K\pi\pi}^2$ projection shows phase space for $K+d \to K+\pi+\pi+d$, the dotted curve that for $K+d \to K^* + \pi+d$. The dotted line joining the two projections shows that $M_{K\pi\pi}^2$ would have to be less than 1.8 $(BeV)^2$ if the "momentum-transfer filter" produced by the deuteron form factor were approximated by a sharp cutoff at 0.2 $(BeV)^2$.

Butterworth et al. 2.3-BeV/c $K^+d \rightarrow K^{*0} + \pi^+ + d$
$\quad\quad\quad\quad\quad\quad\quad\quad\quad\quad \hookrightarrow K^+ + \pi^-$

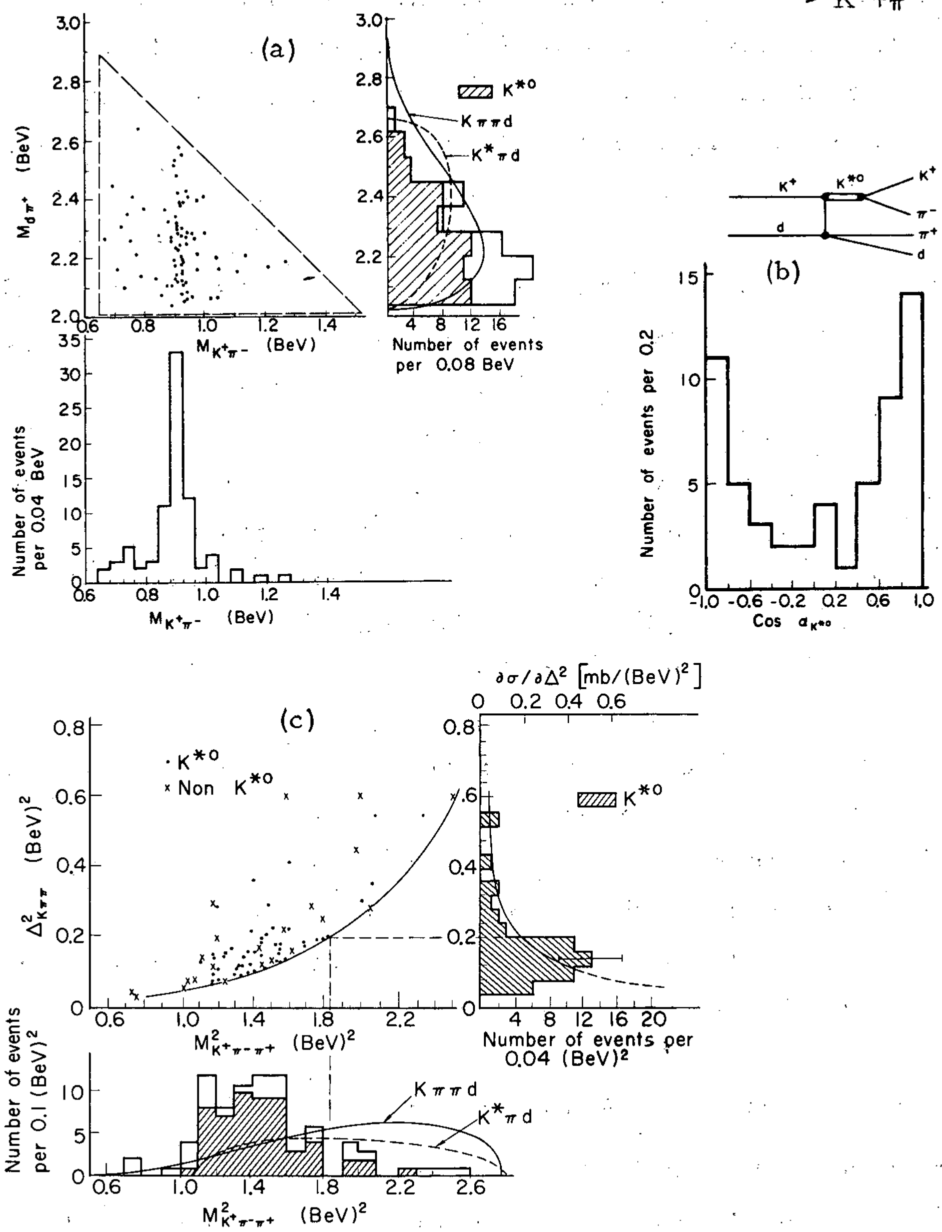

MUB-10194

three-particle system. The Chew-Low plot boundary then forces these events to occur at low mass values. This might be considered as a trivial explanation of the effect.

(b) A virtual pion may be scattered off the deuteron, leaving a $\pi^{\pm}d$ structure whose mass corresponds roughly to formation by one of the nucleons in the deuteron of an $N^{*++}(1238)$ or $N^{*-}(1238)$ without deuteron breakup. In this case we are dealing with virtual pion exchange in accordance with the Drell process, which gives rise to a broad $\rho\pi^{\pm}$ (or $K^{*}\pi$) enhancement. On this interpretation the observed alignment of the ρ^{0} (or K^{*}) can be understood as well.

(c) Coherent production of a 1^{+} state would also lead to alignment of the ρ^{0} (or K^{*0}), as discussed in the previous section. In this case the question arises why the A_1[or $K^{**}(1320)$] if they are indeed 1^{+} mesons do not show up. One possibility here is that the coherent process actually enhances a 1^{+} nonresonant state! As has been reemphasized recently,[49] the coherent process will primarily excite states which can be produced with exchange of angular momentum only. Thus for a 0^{-} incident particle and $\ell^{P}=0^{+}, 1^{-}, 2^{+}, \cdots$, we get states with $J^{P} = 0^{-}, 1^{+}, 2^{-}, \cdots$ formed. Of these the 0^{-} state corresponds to "elastic" diffraction scattering, while the 1^{+} state is the first more complex coherent state beyond diffraction scattering.

If either (b) or (c) is the correct interpretation here it is very likely that this process also contributes to the "coherent" scattering observed in the heavy-liquid chamber.[1] In fact the entire A_1 phenomenon observed in that experiment could be of this nature. An obvious test here would be to study the π^{-} and K^{+} interactions leading to three bosons in a heavy-liquid chamber as a function of incident momentum.

VIII. SUMMARY AND CONCLUSION

We summarize the tests discussed here in Table II.

There appears little doubt that in both cases discussed here the Deck mechanism plays an important role. The real question boils down to this: is there a resonance in addition to the kinematical enhancement effect? The principal evidence favoring this assumption is the extremely sharp A_1 peak observed in the data of Deutschmann et al.[7] on the 8-BeV/c

Table II. Tests on the A_1 and K^{**}(1320).

Test	Predictions for: A_1 or K^{**} by Deck mechanism	Predictions for: A_1 or K^{**} as 1^+ meson	Experimental results: A_1 band	Experimental results: K^{**} band	Experimental results: A_2 band for control
$\pi\pi$ (or KK) scattering angle	$\cos^2\alpha$	$\approx \cos^2\alpha$	$\cos^2\alpha_{\pi\pi}$ with asymmetry	$\cos^2\alpha_{KK}$	$\approx$ Isotropic
T-Y angle at ρ^0 (or K^*) vertex	Isotropic	$\approx$ Isotropic	Isotropic	Isotropic	$\approx$ Isotropic
T-Y angle at πp vertex	Isotropic	?	Nonisotropic	Nonisotropic	Nonisotropic
			[Explained by overconstraints on system]		
$\Delta^2(\rho)$ [or $\Delta^2(K^*)$]	"Consistent with OPE"	Probably broader than OPE	Δ^2 peak 0-30 m_π^2	Δ^2 peak 0-40 m_π^2	Double "hump"
			[Width "explained" by Chew-Low boundary]		
$d^2\sigma/d\Omega dM$	$\approx \left(\frac{d\sigma_{el}}{d\Omega}\right)$	?	$\approx \frac{d\sigma_{el}}{d\Omega}$	$\approx \frac{d\sigma_{el}}{d\Omega}$	——
			[Without $\pi\rho$ or πK^* constraint]		
Asymmetry in ρ^0 (or K^*) decay	Same asymmetry as for free ρ^0 (or K^*) decay	No asymmetry	Asymmetry present	Slight asymmetry	No asymmetry
ρ^0 (or K^*) direction in A_1 (or K^{**}) c.m.	?	Isotropic	Small $\approx \cos^2$ term present	Small $\approx \cos^2$ term present	Small $\approx \cos^2$ term present

The symbol "≈" means that the behavior can be approximated by the quantity shown.
The symbol "?" means that we have not computed the corresponding distribution.

$\pi^+ p$ reaction and the similar sharp $K^*(1320)$ peak observed by us[11] in the 4.6-BeV/c K^+p reaction. If these peaks persist with improved statistics (although it is not obvious at present that they will), it may become possible to perform the tests described here on a select sample of events from the narrow peaks. Thus we feel that considerably more data will be required before the presence of bona fide mesons can be either established or completely ruled out.

We wish to acknowledge the help and effort contributed by Dr. Benjamin C. Shen to all phases of this work. We wish to thank Dr. Janos Kirz and Professor George H. Trilling for a number of discussions and helpful comments on this work.

We also wish to acknowledge the help and hospitality offered to us by Professor Alladi Ramakrishnan and the other members of the Institute of Mathematical Science in Madras, India, during our all-too-brief stay there.

This work was done under auspices of the U. S. Atomic Energy Commission, and, for one of us (SG), of the John S. Guggenheim Foundation.

REFERENCES

1. J. F. Allard, D. Drijard, J. Hennessy, R. Huson, A. Lloret, P. Musset, J. J. Veillet, H. H. Bingham, M. Dickinson, R. Diebold, W. Koch, D. W. G. Leith, M. Nikolic, B. Ronne, G. Bellini, E. Fiorini, P. Negri, M. Rollier, J. Grussard, J. Ginestet, A. H. Tran, M. DiCorato, W. B. Fretter, J. H. Lubatti, and W. Michael, Phys. Letters 12, (1964).
2. G. Goldhaber, J. L. Brown, S. Goldhaber, J. A. Kadyk, B. C. Shen, and G. H. Trilling, Phys. Rev. Letters 12, 336 (1964).
3. S. U. Chung, O. I. Dahl, L. M. Hardy, R. J. Hess, G. R. Kalbfleisch, J. Kirz, D. H. Miller, and G. A. Smith, Phys. Rev. Letters 12, 621 (1964).
4. Aachen-Berlin-Birmingham-Bonn-Hamburg-London-Munchen Collaboration, Phys. Letters 10, 226 (1964).
5. J. Alitti, J. P. Baton, B. Deler, M. Neveu-Rone, J. Gussard, J. Ginestet, A. H. Tran, R. Gessaroli, and A. Romano, Phys. Letters 15, 69 (1965).
6. V. E. Barnes, W. B. Fowler, K. W. Lai, S. Orenstein, D. Radojicic, and M. S. Webster, Phys. Rev. Letters 16, 41 (1966).
7. M. Deutschmann, R. Steinberg, H. Weber, W. Woischnig, V. Belyakow, C. Grote, J. Klugow, S. Nowak, S. Brandt, V. T. Cocconi, O. Czyzewski, P. F. Dalpiaz, E. Flaminio, H. Hromadnik, G. Kellner, and D. R. O. Morrison, Phys. Letters 20, 82 (1966).
8. G. Bozóki, E. Fenyves, E. Gombosi, and E. Nagy, Phys. Letters 18, 206 (1965).
9. M. L. Good and W. D. Walker, Phys. Rev. 120, 1857 (1960).
10. S. P. Almeida, W. H. Atherton, T. A. Byer, P. J. Dornan, A. G. Forson, J. H. Scharenguivel, D. M. Sendall, and B. A. Westwood, Phys. Letters 16, 184 (1965).
11. S. Goldhaber, J. L. Brown, I. Butterworth, G. Goldhaber, B. C. Shen, C. M. Fu, and G. H. Trilling, K^+p Interaction at 4.6 BeV/c, Lawrence Radiation Laboratory Report UCRL-16332, Feb. 1966 (unpublished),

presented by S. Goldhaber at the Oxford International Conference on Elementary Particles on Sept. 19-25, 1965, Abstract A-160.

12. W. De Baere, J. Debaisieux, P. Dufour, F. Grard, J. Houghebaert, L. Pape, P. Peeters, F. Verbeure, R. Windmolders, T. A. Filippas, R. George, Y. Goldschmidt-Clermont, V. P. Henri, B. Jongejans, W. Koch, G. R. Lynch, D. W. G. Leith, F. Muller, and J. M. Perreau, The Enhancement ($K\pi\pi$) Around 1270 MeV/c^2 in the Reaction $K^+p \rightarrow KN\pi\pi$ at 3.0, 3.5, and 5 GeV/c, presented at the Oxford International Conference on Elementary Particles, Sept. 19-25, 1965, Abstract A.127.
13. Review talk on mesons by A. H. Rosenfeld at the 1965 Oxford Conference – to be published in the supplement to the Proceedings of the Conference.
14. S. L. Glashow and R. H. Socolow, Phys. Rev. Letters 15, 329 (1965).
15. J. M. Bishop, A. R. Erwin, and W. D. Walker, in Proceedings, Second Topical Conference on Resonant Particles, Ohio University, Athens, Ohio, 1965, B. A. Munir, Editor (Ohio University Press, Athens, 1965) p. 184
16. S. U. Chung, O. I. Dahl, L. M. Hardy, R. I. Hess, L. D. Jacobs, J. Kirz, and D. H. Miller, Phys. Rev. Letters 15, 325 (1965).
17. M. Derrick, Bull. Am. Phys. Soc. 11, 76 (1966).
18. M. Nauenberg and A. Pais, Phys. Rev. Letters 8, 82 (1962).
19. R. F. Peierls, Phys. Rev. Letters 6, 641 (1961).
20. C. Goebel, Phys. Rev. Letters 13, 143 (1964).
21. R. T. Deck, Phys. Rev. Letters 13, 169 (1964).
22. U. Maor and T. A. O'Halloran, Jr., Phys. Letters 15, 281 (1965).
23. M. Month, Phys. Letters 18, 357 (1965).
24. N. P. Chang, Phys. Rev. Letters 14, 806 (1965).
25. Quoted by G. Goldhaber in Second Coral Gables Conference on Symmetry at High Energy, University of Miami, 1965, B. Kursunoglu, A. Perlmutter, and I. Sakmar, Editors (W. H. Freeman and Co., 1965), p. 34.
26. Aachen-Berlin-Birmingham-Bonn-Hamburg-London (I. C.) – Munchen Collaboration, Phys. Rev. 138, B897 (1965).
27. L. Seidlitz, O. I. Dahl, and D. H. Miller, Phys. Rev. Letters 15, 217 (1965).
28. M. A. Abolins, D. D. Carmony, R. L. Lander, Ng. H. Xuong, and P. M. Yager, in Proceedings, Second Topical Conference on Resonant Particles,

Ohio University, Athens, Ohio, 1965, B. A. Munir, Editor (Ohio University Press, Athens, 1965) p. 198.

29. H. O. Cohn, W. M. Bugg, and G. T. Condo, Phys. Letters 15, 344 (1965).

30. B. C. Shen, G. Goldhaber, S. Goldhaber, and J. A. Kadyk, Phys. Rev. Letters 15, 731 (1965).

31. S. D. Drell, Phys. Rev. Letters 5, 342 (1960); Rev. Mod. Phys. 33, 458 (1961).

32. J. F. Allard, D. Drijard, J. Hennessy, R. Huson, A. Lloret, J. J. Veillet, G. Bellini, M. Di Corato, E. Fiorini, P. Negri, M. Rollier, J. Crussard, J. Ginestet, A. H. Tran, H. H. Bingham, R. Diebold, W. B. Fretter, H. J. Lubatti, W. Michael, and K. Moriyasu, Phys. Letters 19, 431 (1965).

33. F. R. Huson, Bull. Am. Phys. Soc. 11, 54 (1966).

34. H. Bingham, R. Huson, K. Moriyasu, and J. Six, on the work by the Orsay-Ecole Polytechnique-Milan-Saclay-Berkeley Collaboration, private communication.

35. T. Ferbel, Production of A_1, A_2, and B Mesons in High-Energy $\pi^{\pm}$ Interactions, University of Rochester, Rochester, N. Y. (to be published).

36. A. S. Goldhaber (University of California, Berkeley, California), private communication.

37. Cambridge Bubble Chamber Group–Talk by U. Maor, in Proceedings, Second Topical Conference on Resonant Particles, Ohio University, Athens, Ohio, 1965, B. A. Munir, Editor (Ohio University Press, Athens, 1965) p. 476.

38. G. Goldhaber, J. L. Brown, I. Butterworth, S. Goldhaber, A. A. Hirata, J. A. Kadyk, B. C. Shen, and G. H. Trilling, Phys. Letters 18, 76 (1965).

39. P. J. Dornan, V. E. Barnes, B. B. Colwick, P. Guidoni, G. R. Kalbfleisch, R. B. Palmer, D. Radojicic, D. C. Rahm, R. R. Rau, C. R. Richardson, N. P. Samios, I. O. Skillicorn, B. Goz, M. Goldberg, T. Kikuchi, and J. Leitner, Bull. Am. Phys. Soc. 11, 342 (1966).

40. C. Zemach, Phys. Rev. 133, B1201 (1964).

41. W. R. Fraser, J. R. Fulco, and F. R. Halpern, Phys. Rev. 136, B1207 (1964).

42. R. Diebold, Dalitz Plot Density Along the ρ Band of π-p Resonance, CERN/TC/PROG 64-25, Nov. 1964 (unpublished).

43. D. Leith (CERN), private communication.

44. G. Wolf, quoted in Ref. 7.

45. D. H. Miller, L. Seidlitz, and O. I. Dahl, Bull. Am. Phys. Soc. 11, 59 (1966); also L. Seidlitz, O. I. Dahl, D. H. Miller, in Proceedings, Topical Conference on Resonant Particles, Ohio University, Athens, Ohio 1965, B. A. Munir, Editor (Ohio University Press, Athens, 1965) p. 162.

46. M. A. Abolins, D. D. Carmony, R. L. Lander, and N. Xuong, Phys. Rev. Letters 15, 125 (1965).

47. G. Vegni, H. Winzeler, P. Zaniol. P. Fleury, and G. De Rosny, Phys. Letters 19, 526 (1965).

48. I. Butterworth, G. Goldhaber, S. Goldhaber, A. A. Hirata, J. A. Kadyk, and G. H. Trilling, Phys. Rev. Letters 15, 500 (1965).

49. A. S. Goldhaber and M. Goldhaber, in Preludes in Theoretical Physics in Honor of V. F. Weisskopf; Editors A. DeShalit, H. Feshbach, and L. Van Hove (North-Holland Publishing Company, Amsterdam, 1965), p. 313.